WIRELESS SENSOR NETWORK FOR MONITORING OF HISTORIC STRUCTURES UNDER REHABILITATION

A Thesis

by

JULIE MARIE SAMUELS

Submitted to the Office of Graduate Studies of
Texas A&M University
in partial fulfillment of the requirements for the degree of

MASTER OF SCIENCE

December 2010

Major Subject: Civil Engineering

Wireless Sensor Network for Monitoring of Historic Structures under Rehabilitation

WIRELESS SENSOR NETWORK FOR MONITORING OF HISTORIC STRUCTURES UNDER REHABILITATION

A Thesis

by

JULIE MARIE SAMUELS

Submitted to the Office of Graduate Studies of
Texas A&M University
in partial fulfillment of the requirements for the degree of

MASTER OF SCIENCE

Approved by:

Chair of Committee,	Stefan Hurlebaus
Committee Members,	Joseph M. Bracci
	David G. Woodcock
	Gary T. Fry
Head of Department,	John Niedzwecki

December 2010

Major Subject: Civil Engineering

ABSTRACT

Wireless Sensor Network for Monitoring of Historic Structures under Rehabilitation.

(December 2010)

Julie Marie Samuels, B.S., Texas A&M University

Chair of Advisory Committee: Dr. Stefan Hurlebaus

The use of a wireless sensor network (WSN) to monitor an historic structure under rehabilitation is the focus of this research. To thoroughly investigate the issue, two main objectives are addressed: the development of a reliable WSN tailored for use in historic structures, and the implementation of the monitoring system in the field to test the feasibility of the WSN and its applicability for structural health monitoring (SHM).

Three field studies are undertaken in this research. The Frankford Church, an historic wooden church which required foundation replacement, is the first field study. Sensors monitor tilt of the church's walls throughout construction. During the construction process, the entire floor of the church is removed and the tree stump foundations are replaced by concrete masonry unit (CMU) blocks and steel pedestals. The tilt in the walls is correlated to the construction process. St. Paul Lutheran, an historic masonry church with timber-framed roof, constitutes the second field study. In this structure, the foundations along the exterior walls are underpinned and the floors are removed and replaced with a floating concrete slab. Detected movements are also correlated to the construction efforts. The Johanniskirche, an historic masonry church

with moisture problems, is the final field study case. Real-time and past measured WSN climate data is used to determine the most appropriate solution for the humid climate and resulting condensation problems in this structure. From these results, a moisture migration risk analysis protocol is created for use with a WSN to address condensation issues.

The results of the tilt monitoring indicate that the approach is realistic to monitor tilt in the walls of historic structures. For future research, it is recommended to implement motes with higher tilt sensitivity. Also, further development of energy saving algorithms and energy harvesting methods will improve the WSN's performance.

Climate monitoring results show it is feasible to monitor climate conditions of historic structures. The moisture migration protocol provides a basis for further improvement. Implementation of this tool will help predict condensation events and prevent future damage to the historic structure.

ACKNOWLEDGEMENTS

I would like to thank my committee chair, Dr. Hurlebaus, for his guidance and mentorship. I would also like to thank my committee members, Dr. Bracci, Prof. Woodcock, and Dr. Fry, for their inspiration and support throughout the course of this research.

Thanks to Michael Reyer for his patience and guidance with the Crossbow Wireless Sensor Network. His help was invaluable to the completion of this research. Also, thank you to Mark Bolding for his support and help with the wireless sensor network and to Bill Samuels and Gigi Kalmon for their help installing the wireless sensor network and changing batteries.

I also wish to thank Steve Lucy from Jaster-Quintanilla for allowing me to use two of their historic preservation projects: Frankford Church and St. Paul Lutheran to test the wireless sensor network. My appreciation goes to John Walter and Howard Nedderman from Nedderman & Associates for their help during the rehabilitation process at the Frankford Church. Thanks also go to Pastor Schmidt and the St. Paul Lutheran congregation for allowing me to install the wireless sensor network on their beloved structure. Without their help, this research would not have been possible.

I also want to extend my gratitude to the DAAD RISE Professional Program and the MPA at the University of Stuttgart for providing funding for my research internship at the MPA in Stuttgart, Germany. I would like to recognize and thank Dr. Markus Krüger and Dr. Christian Grosse for organizing my research in Germany and for their

support. Also, thanks to Frank Lehmann and Sebastian Bachmaier for their help with my research in Germany. Additionally, I would like to thank Lotte Hurlebaus and her family for making me feel welcome my first few weeks in Germany.

Finally, thanks to my family for their love and encouragement throughout this process.

TABLE OF CONTENTS

LIST OF FIGURES

Page

Page

LIST OF TABLES

CHAPTER I

INTRODUCTION

Historic structures are designated and treated separately from other existing structures due to the restrictions imposed by both the National Park Service and the Secretary of the Interior's Standards. Typically, if a structure is over 50 years old and can demonstrate that it is of historical significance, then it is eligible for entry into the National Register of Historic Places, maintained by the National Park Service. The advantage of having a structure that qualifies for the National Register is that financial incentives (such as tax credits and federal grants) exist for the treatment and upkeep of the structure. Ideally, if a structure is placed on the National Register, work should then follow the guidelines set forth by the Secretary of the Interior's Standards for any treatments. As one can imagine, the treatment criteria for a registered historic structure should be much more strictly monitored than the treatment of another non-historic structure due to the strong desire to protect the historical significance. The *Secretary of the Interior's Standards for the Treatment of Historic Properties* detail, through written descriptions as well as pictures, the acceptable treatments for historic structures. For the solution to be relevant, the approach must not have a negative impact on the historic character of the property (Weeks and Grimmer 1995).

On an even larger scale than in the US, Europe has a wealth of historic structures due to its ancient roots and love of fine architecture throughout the ages. It is vital that

---

This thesis follows the style of *Journal of Structural Engineering.*

these structures, as well as those in the US, be preserved when at all possible because they represent a major part of a country's cultural heritage. Each country has its own interpretation of the various architectural styles, which makes every structure unique and of great value. As noted by Blaise et al. (2008), "heritage sites match the interests of many in that they materialize historical influences and differences".

A prime example of an historic structure which could have benefitted from the use of monitoring is the Virginia State Capitol, which was renovated and added to in 2005. Figure 1-1 depicts the Virginia State Capitol after the expansion project was complete. This property is listed on the National Register of Historic Places, and therefore falls under the jurisdiction of the Secretary of the Interior's Standards for Historic Preservation. The original structure, built in 1785, was designed by Thomas Jefferson and is still the seat of government for the Commonwealth of Virginia. The scope of this project included replacing mechanical, electrical and heating, ventilation and air conditioning (HVAC) systems, preventing water penetration, restoring architectural details, renovating exterior surfaces, and the construction of a 27,000 square-foot underground expansion to bring the building up to Americans with Disabilities Act (ADA) standards (Fisher 2005). As can be seen in Figure 1-2, taken after the underground addition was completed, severe cracks appeared in the foundation under a column of the primary structure. In this case, glass tell-tales were affixed to the crack to detect any additional foundation shifts. This cracking may have been predicted if a wireless sensor network was in place to actively monitor the building during construction, allowing corrections to be made as the work proceeded. The use of

monitoring of the deep excavations adjacent to the Texas State Capitol's below-grade extension allowed immediate detection of movement and work was halted to allow installation of additional rock anchors.

Figure 1-1. Virginia State Capitol after expansion (Staley 2008)

Figure 1-2. Cracking of foundation under column at Virginia State Capitol (Staley 2008)

Of particular importance to structural engineers and heritage conservationists alike is the development of a reliable wireless sensor network (WSN) that will increase knowledge of the behavior of many historic structures. Since many historic structures are made out of older building materials, there are many unknown material properties which make building assessment difficult. In addition, there are many hidden defects that could be detected much more quickly with applied WSN technology. This can help not only with the analysis of the physical structural integrity, but also moisture migration in the walls which can damage wall decoration and plaster, and in extreme cases, lead to structural instability. Having an effective and reliable WSN to collect building response data will help structural engineers more quickly and easily understand the current and changing conditions of the overall structure. Instead of relying completely on assumed material conditions or a multitude of smaller material tests, structural engineers will be able to quickly and cost effectively use data obtained from a WSN to evaluate the overall condition of a historic structure.

While some wireless sensor monitoring of structural health is currently being done across the country, the networks are very limited in terms of their size and effectiveness (Swartz et al. 2005). In addition, more research must be performed when working with historic structures in particular due to the additional concerns and regulations imposed by the National Park Service and the Secretary of the Interior's Standards.

Literature Review

The WSNs must conform to many of the same standards to which the traditional wired networks adhere. Specifically, they must be able to report the structural response and

signify a structural degradation over time. More importantly for historic structures, the WSN must be able to identify major deformations or material fractures that are present (Cinque et al. 2006). The structural engineer can then analyze the data to determine the level of danger that the structure poses to humans.

One example of a WSN system that has already been created for data acquisition of structural responses is detailed in Xu et al. (2004), and it is termed Wisden. This system combines data time-stamping that is independent of a global synchronization and a reliable data transport that utilizes both end-to-end and hop-by-hop data transmission. The three key focuses of the Wisden system are Reliable Data Transport, Compression, and Data Synchronization. These are three key issues that must be addressed before WSNs can become widespread and useful in a variety of applications (Xu et al. 2004). The Wisden system is intended for a rapid and short-term deployment, where battery power is not an issue. This system offers the functionality of a data logger; however it lacks the data processing capabilities of a full data acquisition system. This flexibility allows Wisden to support a variety of different channels, a feat that traditional data loggers cannot claim. In addition, the Wisden system strives to reduce energy usage by compressing data so that it can be processed in the network much faster (Xu et al. 2004).

Ideas for decreasing the cost of a WSN can possibly be obtained by understanding the process used by Bastianini et al. (2007) in creating an autonomous wireless device for structural health monitoring. This device has many self-referenced sensors, communicates with the global system for mobile communication (GSM) network, and is powered completely by batteries (Bastianini et al. 2007). According to

Glaser et al. (2005), advancements in microfabrication of microelectromechanical systems (MEMS) and bioengineered systems have made "powerful, ubiquitous sensing a readily achievable reality". They note that research is currently underway to create a system that "virtually" configures the wireless sensors with new software. This will significantly increase efficiency of installation and implementation, which will in turn cut costs. It has also been asserted that densely populating an area with several low-cost sensors could provide the same results as installing one expensive sensor (Glaser et al. 2005). One optional design for a wireless sensor network that helps solve the power supply problem has been created by Swartz et al. (2005). This paper includes information on a new design that utilizes a four layer circuit board as opposed to a two layer board, which was often used previously for the network. According to this information, the four layer board provides for a separation of the power supply and the ground that is more optimal for both the analog and digital components involved. This new design reduces power consumption by utilizing a low power radio, improves communication with more accurate time synchronization, and gives greater measurement fidelity (Swartz et al. 2005).

Chen and Lin (2007) contend that battery life is the primary limiting factor for wireless sensor technology. To address this issue, they have proposed a 4D-Fuzzy Petri Net approach which can increase battery power two to five times. This approach cycles through three different states to conserve energy: dormant state, sleeping state and active state (Chen and Lin 2007). Another approach to save battery life is to utilize a multi-scale network, which only activates sub-networks in areas of suspected damage

(Kijewski-Correa et al. 2006). This design also reduces the possibility of interference between sensors by increasing time increments of data collection in areas that do not have perceived damage. In addition, Kijewski-Correa et al. (2006) recommend the idea of coupling strain gages and accelerometers for increased accuracy. The embedment of processors into wireless sensors is a possible option to save battery life. Tanner et al. (2003) found that this alteration was very effective because "one byte of data transmission consumes the same amount of energy as about eleven thousand cycles of computation in the employed hardware platform".

Hollar (2000) developed a variety of small motes, or tiny wireless sensors, which all possessed the following subsystems: power, computation, sensors and communication. The first commercial off-the-shelf (COTS) Dust minimote was 2.54 cm x 2.54 cm x 1.27 cm and was characterized by a radio frequency (RF) transceiver, temperature sensor and an Atmel AVR AT90S2313 microcontroller. The most advanced COTS Dust minimote, weC mote, is 3.81 cm diameter x 1.27 cm and contains an integrated printed circuit board (PCB) antenna, light and temperature sensors and a 4 MHz central processing unit (CPU) clock; however, its best attribute is its ability to be reprogrammed wirelessly. In 2002, an even smaller mote (2.5 mm x 2.5 mm) was developed, called Spec node. Its most impressive feature is that the CPU, memory and RF transceiver are all on a single piece of silicon (Gao and Spencer 2008).

Reyer et al. (2009) designed a WSN for structural health monitoring using commercially available wireless sensors to measure and extract vibration characteristics of bridges. The WSN design considers time synchronization, modularity and flexibility

in post installation usage. They verified the functionality of the network in a laboratory experiment.

Research performed by Bischoff et al. (2007) has also focused on creating a WSN that is intended for long term structural monitoring. The key topics discussed in this research are related to the data processing and data management issues that arise at the network nodes (Bischoff et al. 2007). This research strives to understand and explain these two issues and how they are critically important in developing an effective WSN.

After a general introduction to the concept of WSNs, Lynch and Loh (2006) cover various hardware designs for platforms that are available today. The hardware platforms are broken down into "Academic Wireless Sensing Unit Prototypes" and "Commercial Wireless Sensor Platforms" to present a solid idea of what hardware is currently being developed. It then breaks down various types of embedded software that is available for wireless networks. Additionally, the authors introduce a variety of emerging concepts for using WSNs in the field of structural health monitoring. This paper also includes an informative section on the performance validations of wireless sensors which include the summarized results from a very wide range of research projects relating to WSN technology in structural health monitoring.

While the reliability of a WSN is of critical importance, there are also a few other key goals that must be reached to ensure adequate performance of widespread WSNs. The goals stated here have been previously determined by Swartz et al. (2005). However, it is important to remember each of these criterion with this adaptation of the WSN. As mentioned above, the cost is of utmost importance due to the fact that

outfitting a structure with a wireless network would enable a much denser population of sensors (as compared to a wired system). Therefore, if the cost is too high then the technology will never become widespread. Secondly, the wireless network must be able to operate without consuming a significant amount of energy since each unit will have to be battery powered. In addition, the range of communication for each sensor must be adequate so that each sensor can easily interact and communicate with any other unit in the network. This issue is critical for an effective system, and creating a wireless system will make this task more difficult than it has previously been. Lastly, it is important to make sure that the technology is fully scalable so that the size of the system is not a restriction for any structure.

With the increasing availability of smaller and more affordable sensors, the reliability of the sensor network will most likely be the limiting factor in developing the appropriate system for use in historic structures. The best wireless network system will be the one that can be installed with limited to no damage to the structure while still being able to provide accurate, time-sensitive measurements on a consistent basis (Cinque et al. 2006). Just as in the research performed by Cinque et al. (2006), three key requirements tested with this research are (i) obtaining measurement synchronization that is reliable, (ii) delivering a large amount of measurements in a reliable manner, and (iii) minimizing the amount of human intervention within the network. Each of these three qualities is essential to the effectiveness of any WSN, especially in an historic structure that may be on the verge of failure.

With respect to the future applicability of wireless sensors for use in structural health monitoring, Tanner et al. (2002, 2003) used a Mica mote to detect a loose bolt by measuring the acceleration response of the beam on both sides of the joint and calculating the correlation coefficient. In addition, Sohn et al. (2002) installed sensors at each degree of freedom and combined an AR-ARX (auto-regressive and auto-regressive with exogenous inputs) model, nonlinear principle component analysis and statistical analysis to successfully identify damage locations in an eight degree of freedom experimental system impacted by environmental changes. Also, Hocker (2010) installed sensors on a salvaged 17th Century warship to carefully monitor climate conditions throughout the hull in order to prevent further deterioration of the wood.

Technical Needs

At this point, it can be seen that much research has been performed on the idea of using WSNs for structural health monitoring; however, there has been no or only little research relating the use of WSNs with the concerns that are present in historic structures.

In addition to addressing the above concerns with the current WSNs available, research is needed to provide information related to the optimal placement of sensors on the historic structure of interest. This optimal location decreases the cost of installation while increasing the reliability of the network itself (Cinque et al. 2006). Although this idea of determining the optimal placement location is not new in itself, there is currently a lack of widespread data on optimal sensor placements for historic structures. Therefore, additional research into this area is needed.

Furthermore, some of the most successful projects involving WSNs still lack long-term reliability and power options which are two issues that will be evaluated in this research. Efforts are needed to utilize wireless sensors which incorporate energy scavenging devices such as piezoelectric elements, thermocouples, or solar cells. This can significantly increase the battery life and capabilities of the sensors (Hurlebaus and Gaul 2006). Reinisch et al. (2007) notes that node visibility is a potential drawback to wireless sensors, i.e.: nodes A and B can see node C, but not each other. Another issue to be aware of is the potential for a wireless network channel to be jammed due to other devices utilizing the same frequency.

Objectives

The primary goal of this research is to provide a reliable solution for monitoring of a historic structure in a non-destructive and cost effective way using a WSN. The WSN technology will be developed such that the sensors will be able to measure structural response to both man-made and natural forces in order to determine the safety of the structure and hopefully prevent any catastrophic failures. The objectives of this study are to (i) develop a reliable WSN that is tailored for use in historic structures, and (ii) implement the monitoring system in the field to test the feasibility of the WSN and its applicability for structural health monitoring.

Structure of Thesis

The thesis is structured as follows. After a brief introduction to wireless sensor networks, the WSNs used in the three case studies are described. From there, each field study is detailed in a separate section. Each section will begin with a brief history of the historic

structure, followed by the rehabilitation work, monitoring and results. Finally, the conclusion is presented, including suggestions for future research efforts.

CHAPTER II

WIRELESS SENSOR NETWORK

The purpose of the wireless sensor network is to collect data from individual sensors and compile it for later analysis. Advantages of a WSN include greater flexibility, and ease of installation; however, it is limited by available power sources and the possibility of environmental conditions impacting the data transmission process. The sensors of a WSN can be placed at any location desired while only being limited by the transmission distance capacity of the radio transmitter and transmission barriers such as metal and thick concrete walls. In addition, once the sensors are in place, more can be easily integrated into the network. With the increasing research in the field of WSNs, the availability of sensors is improving and their cost is decreasing. Currently, wireless sensors are approximately the same price as wired sensors. However, there is a significant decrease in the installation cost of WSNs.

As was previously mentioned, battery longevity is a primary limiting factor of WSNs. Much work is underway to develop better, more efficient methods of harvesting energy to increase the capabilities of wireless solutions. Some proposed options include the use of more efficient batteries, and/or harvesting energy using solar, thermal or vibration energy.

The research for this thesis consists of three case studies: Frankford Church, St. Paul Lutheran, and the Johanniskirche. The Frankford Church and St. Paul Lutheran are field studies of the WSN manufactured by Crossbow, whereas the Johanniskirche

utilizes a WSN manufactured by SmartMote to investigate analysis options and develop risk criteria for moisture migration. Therefore, Section 2.1 details the Crossbow WSN implemented at the Frankford Church and St. Paul Lutheran, while Section 2.2 provides information on the SmartMote WSN implemented at the Johanniskirche.

Crossbow WSN

Three key components comprise the WSN: data collection, data accumulation, and data analysis (Figure 2-1).

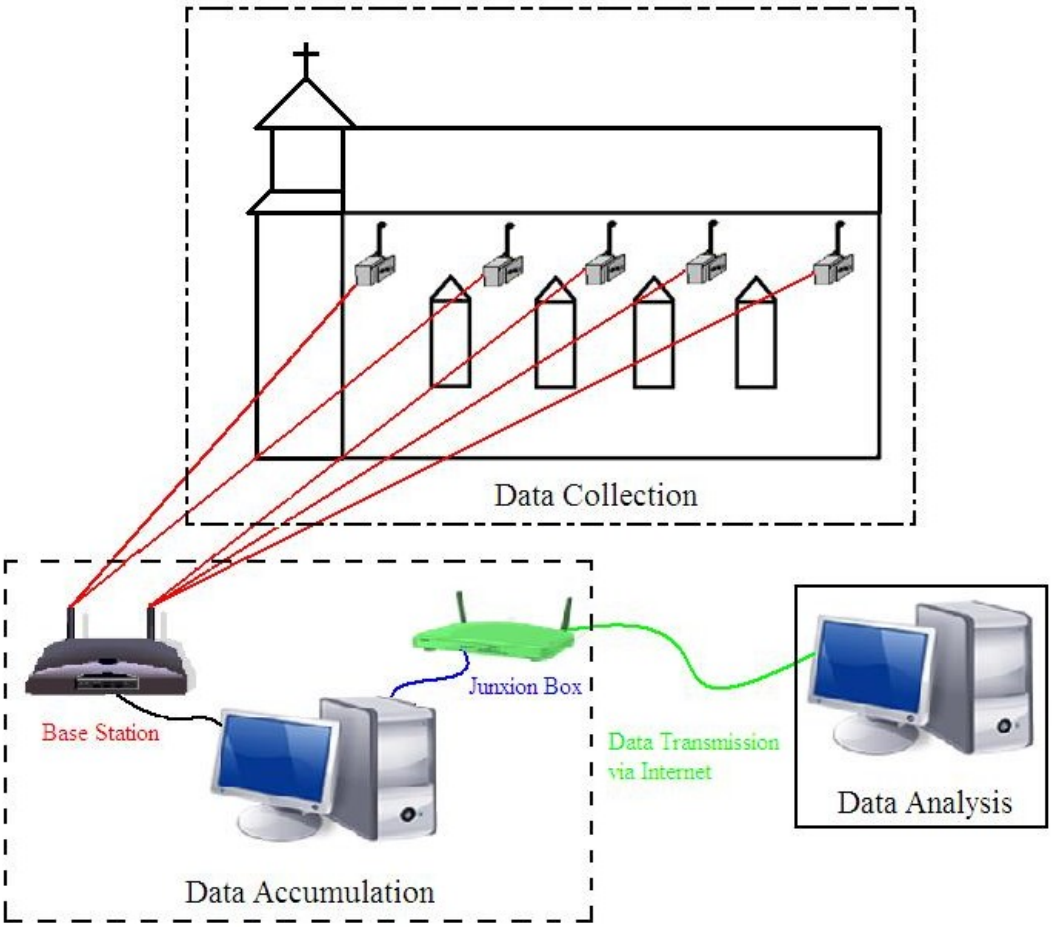

Figure 2-1. Wireless sensor network

Data collection is achieved by connecting a wireless transmission module to a sensor module (comprising a complete mote), which are then attached to a structure. There are several brands and types of motes available both for commercial and research applications. This section describes the Crossbow Mica2 series motes, which utilize TinyOS, a wireless sensor mote operating system that is easily adaptable for specific applications with MTS310 sensor boards as seen in Figure 2-2 (Reyer 2007). The sensor boards are equipped with an Analog Devices ADXL202E dual-axis accelerometer, which utilizes open loop acceleration measurement architecture (Analog Devices 2000). According to the data sheet, "an output circuit converts analog signal to a duty cycle modulated (DCM) digital signal for each axis, which can be decoded with a counter/timer port on a microprocessor". This accelerometer can measure accelerations of at least ± 2g.

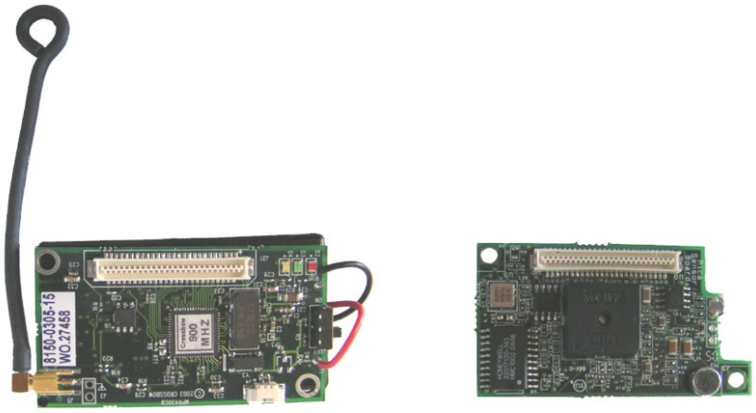

Figure 2-2. Mica2 mote (left) and MTS310 sensor board (right)

After the measurements are taken, the next component of the WSN is implemented. In this stage, the wireless motes send the collected data to the base station using radio transmission. Due to the need for communication between the wireless motes and the base station, a basic star topology is used to implement this network (Figure 2-3). Under this configuration all motes are wirelessly connected to the base station and are given the same priority level. All wireless motes can communicate with the base station. Therefore, individual motes can try to send data packets to the base station at the same time. For this reason, the motes are programmed to continue attempting to send their data until the base station confirms receipt of the data. Once data acquisition has been confirmed, the mote will go into sleep mode and wait a user-defined amount of time to take another measurement. While in sleep mode the mote conserves energy, thus greatly increasing battery life. To allow the user to monitor the WSN from any location, the computer is connected to LogMeIn.com, a remote access website. Constant internet access is provided using a Junxion Box access point with an AT&T Global System for Mobile Communications (GSM) wireless laptop card, which is connected via an Ethernet cable to the computer in the field (Figure 2-1).

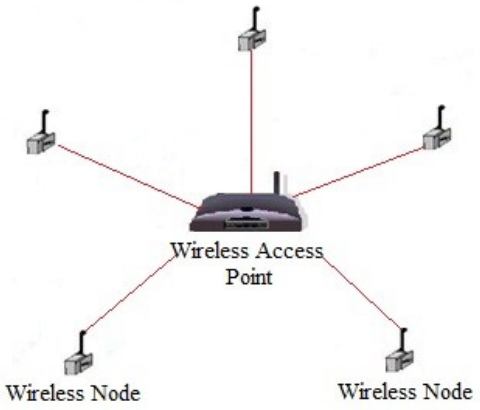

Figure 2-3. Star topology

For data acquisition, the other half of data accumulation, the base station stores the collected data in file that contains the mote number, date and time of measurement, and the raw acceleration values in the $x-$ and $y-$coordinates.

The final aspect of the WSN is data analysis. While the WSN is in the field, the file can be e-mailed and saved to a personal computer. Data is then imported into Matlab and plotted to determine the angle of tilt in the structure. The data that is accumulated by the base station provides raw data that must be calibrated before it is analyzed. The acceleration values can be calculated using (Reyer 2007)

$$\delta_{x,y} = \frac{raw_{x,y}(+g) + raw_{x,y}(-g)}{2} \tag{2.1}$$

$$f_{x,y} = \frac{2[g]}{\left| raw_{x,y}(+g) - raw_{x,y}(-g) \right|} \tag{2.2}$$

$$a_{x,y} = (raw_{x,y} - \delta_{x,y}) * f_{x,y} \tag{2.3}$$

where $\delta_{x,y}$ = calibration offset; $raw_{x,y}(+g)$ = average raw data value for the mote in the positive g orientation in the $x-$ and $y-$ directions (Figure 2-4); $raw_{x,y}(-g)$ = average raw data value for the mote in the negative g orientation in the $x-$ and $y-$ directions (Figure 2-4); $f_{x,y}$ = calibration factor; $a_{x,y}$ = mote acceleration in the $x-$ and $y-$ directions, respectively (units of g). From this, the angles of tilt can be calculated using (Bryson et al. 2009; Analog Devices 2000)

$$\theta_{x,y} = \sin^{-1}\left(\frac{a_{x,y}}{1g}\right) \tag{2.4}$$

where $\theta_{x,y}$ = angle from the horizontal axis; $a_{x,y}$ = mote acceleration in the $x-$ and $y-$ directions, respectively (units of g).

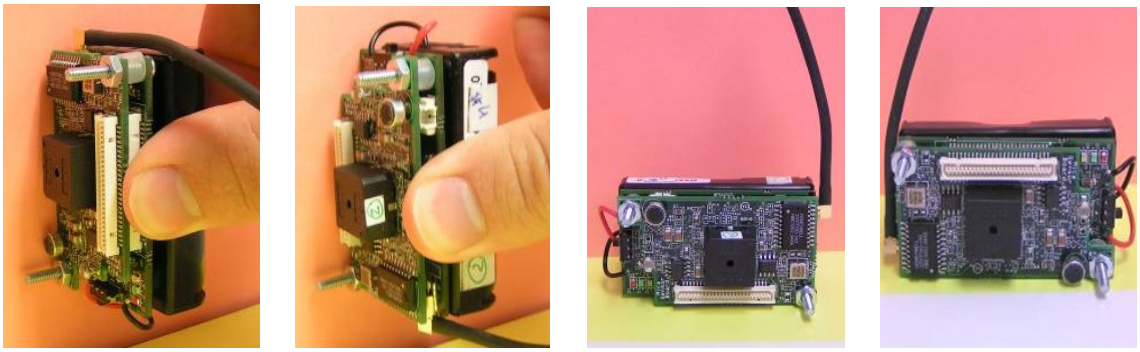

Figure 2-4. Position 1: $raw_y(+g)$, position 2: $raw_y(-g)$ position 3: $raw_x(+g)$ and position 4: $raw_x(-g)$ (left to right)

To calibrate the motes, each mote is programmed to take static measurements at 2 second increments and placed in each of the four positions (Figure 2-4) for 30 seconds

per position. The raw data values are then averaged to calculated the $raw_{x,y}(+g)$ and $raw_{x,y}(-g)$. Table 2-1 displays the raw data values as well as the $\delta_{x,y}$ and $f_{x,y}$ from Motes 8 and 11 as examples of this process.

Table 2-1. Calibration data for Motes 8 and 11

Mote	*raw y* (+g)	*raw y* (-g)	*raw x* (+g)	*raw x* (-g)	δ_y	δ_x	f_y	f_x
8	456.88	565.96	519.22	412.45	511.42	465.84	0.0183	0.0187
11	455.00	564.64	535.10	425.18	509.82	480.14	0.0182	0.0182

SmartMote WSN

Research at the Johanniskirche utilizes a WSN developed by Krüger et al. (2010) and therefore, the focus is on analysis and real-time structural health monitoring rather than the WSN itself. Therefore, this section includes information on the WSN implemented.

As can be seen in Figure 2-5, the wireless sensor mote is comprised of a low power microcontroller, wireless transceiver, primary batteries, and several sensor boards to adjust to a variety of monitoring requirements. Since historic structures and civil engineering structures in general, often exist in extreme environments, the motes are designed to be dust and water protected and have an operational temperature range of -20°C to 80°C. The mote is also easily adaptable for customized monitoring situations. Several MEMS sensors can be attached to one mote simultaneously because its modular system supports many low power modes of operation (Krüger et al. 2010). The design by Krüger et al. (2010) is compatible with the following sensor boards: signal

conditioning board for interfacing piezo- and polyvinylidene fluoride (PVDF) - sensors for acoustic emission and dynamic analysis, multi-sensor signal conditioning board for strain gages, displacement transducers and pressure cells, combined with temperature/humidity and vibration measurements, an inclination sensor board, an air velocity measurement board for low air speed, and an impedance converter system for electrochemical analysis and impedance spectroscopy.

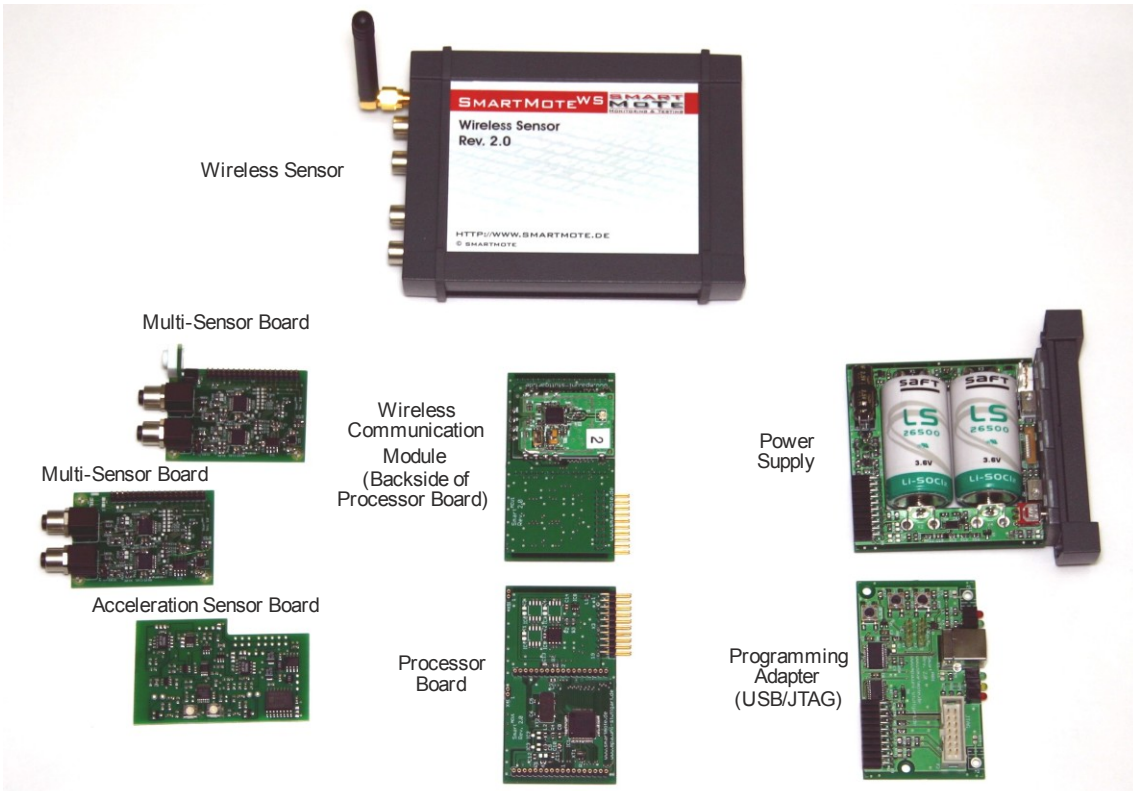

Figure 2-5. Wireless sensor mote components (SmartMote 2010)

For this specific application, a Sensirion SHT15 digital MEMS sensor was used to measure air temperature and humidity. According to Krüger et al. (2010), “the SHT15

digital humidity and temperature sensor is a fully calibrated MEMS sensor that offers high precision, self-calibration functionality and excellent long-term stability". This MEMS sensor has an accuracy of ±0.3°C at 14 bit resolution for temperature and ±2.0% within a range of 10 - 90% at 12 bit resolution for relative humidity.

As previously mentioned, battery life is one of the primary limiting factors. Krüger et al. (2010) designed the SmartMote with this in mind and tested it under a worst case scenario using a data transmission interval of five minutes with the maximum number of data transmissions estimated to be less than 30 μA on average. Extrapolating from this measurement, the 7.7 Ah Lithium Thionyl Chloride Battery ($Li\text{-}SOCl_2$) with a discharge rate of less than 1% per year, could last decades. Although this amount may seem excessive, it was deemed appropriate to provide a large factor of safety so that several sensors can be attached to the mote, some of which will consume much more energy than the test case.

CHAPTER III

FRANKFORD CHURCH: DALLAS, TEXAS (USA)

Frankford Church, a historic wood-framed church (Figures 3-1 & 3-2) in Dallas, Texas, is the subject of this field study. The objective in this case is to measure tilt in the walls of the structure while the foundations are being leveled. A brief history of the historic structure is followed by details of the rehabilitation efforts. Then the monitoring approach is explained and the results are presented.

Historic Structure

This structure, as listed on the Texas Historic Landmarks plaque, was constructed in the 1890s through the efforts of Captain William McKamy and several members of the Frankford community. Although it began as a Methodist Church, it was later occupied by an Episcopalian congregation.

Figure 3-1. Exterior view of Frankford Church

Figure 3-2. Interior view of Frankford Church

Rehabilitation

When it was built, the church was set on a foundation of bois d'arc tree stumps (Figure 3-3). Dallas is a region with very expansive clay soils so over the years the church developed differential settlements of up to 75 mm over approximately 15.25 m. To remedy the problems, the foundations are replaced by concrete masonry unit (CMU) blocks along the interior and steel pedestals on concrete pads under the exterior walls (Figure 3-4). To maintain the appearance of the stump foundations, bois d'arc stumps will be notched to fit around the steel supports. Over the course of the rehabilitation, the structure is leveled several times (Figure 3-3). For minor adjustments, steel pipe supports are connected to the concrete pads using leveling bolts.

Figure 3-3. Original foundations (left) and jacks used to level structure (right)

Figure 3-4. Interior span CMU foundation on concrete pad (left) and exterior span steel pedestal on concrete pad (right)

Monitoring

For this research, each mote is mounted on an angle bracket which is attached with a single 4.76 mm diameter wood screw to the wall approximately 3.66 m above the floor of the church so as to not impede work during the rehabilitation. According to the orientation of the motes on the wall, the local $x-$ axis is perpendicular to the wall, while the local $y-$axis is parallel with the wall. As shown in Figure 3-5, the motes are distributed throughout the church. Motes 5, 6, 11, and 12 are placed directly above the windows.

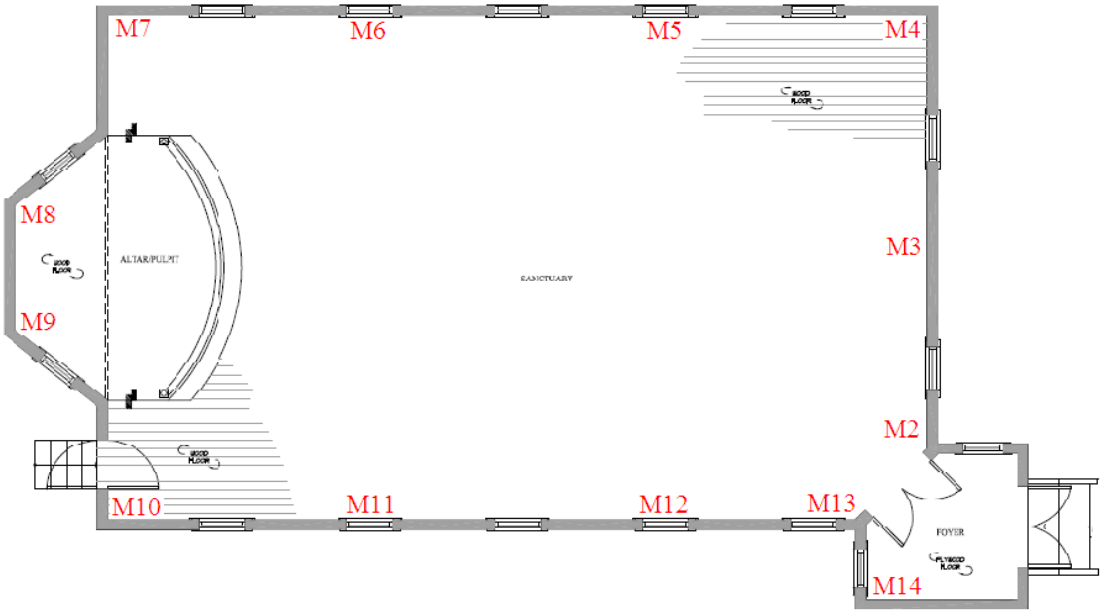

Figure 3-5. Plan view of Frankford Church with mote placement

The base station and desktop computer are set up in the crawl space of the tower at the front entrance to the church. Once all of the equipment is installed, the WSN

programs are started and monitored periodically via remote access for four months. The motes are removed after the foundation issues are resolved.

Results

The WSN is installed eight days before construction began and remains on the structure through the leveling process, until the foundations are in their final locations and only architectural work remains on the interior. Results from each mote are examined for the first eight days to determine if temperature changes could be detected. None of the motes produced data that would indicate temperature dependence. However, it seems plausible that temperature shifts would not be mirrored in the construction materials because the region in which the church is located is prone to a wide range of temperatures. If the material was highly sensitive to such temperature shifts, the structure would have even worse issues than the differential settlements.

For this application, the sensors have a sensitivity of approximately one degree. They do display overall movements throughout construction as a result of leveling and re-leveling the structure. The worst settlement issues occur close to Motes 8 and 11. This is the reason that the results of the motes are chosen as examples (Figure 3-6).

Figure 3-6. Mote 8 (left) and Mote 11 (right)

To confirm that the shifts in the motes are due to external impacts, the results are compared with the construction stages. The construction is divided into ten phases as shown in Table 3-1.

Table 3-1. Construction activities at Frankford Church

Phase	Start Date	End Date	Description
1	8/17/09	8/24/09	Installing WSN
2	8/25/09	9/8/09	Remove pews, base and flooring
3	9/8/09	9/15/09	Start digging up center piers
4	9/15/09	10/2/09	Interior joist and beam repair
5	10/2/09	10/29/09	Rain delay
6	10/30/09	11/2/09	Floor joist repair and addition
7	11/3/09	11/10/09	Work on North beams and level church for the first time
8	11/11/09	11/13/09	Install steel channels around roof line of church for tie rods
9	11/14/09	11/29/09	Rain delay
10	11/30/09	12/19/09	Set steel pedestals, pour concrete pads and jack church up and down until level, remove WSN on 12/19/09

Note that the major spikes in the data occur while the batteries are being changed in each sensor (9/17/09; 10/23/09; 11/13/09; 12/18/09). Mote 8 (Figures 3-7 and 3-8) only had two spikes while Mote 11 (Figures 3-9 and 3-10) has four jumps because the batteries in Mote 8 lost power before they are changed and a static measurement is not taken while the mote is off the wall. Also, the short increments on Figures 3-7 through 3-10 where there are no data points indicate the dates that power outages occur (8/22/09; 8/27/09; 9/8/09; 9/20/09; 9/25/09; 10/4/09). Note that the WSN is not operating after a power outage and it has to be manually reset. The longer increment between October 16th and October 26th represents a loss of battery power. There is a longer range of power loss for Mote 8 because it is furthest from the base station and is programmed to transmit data at a higher RF power, whereas the other motes are programmed for a lower RF power.

The motes indicate more movement in the $y-$direction throughout the construction process. However, it should be noted that each mote follows a similar trend, corresponding to construction. During Phase 1 (8/17/09 to 8/24/09), the measurements remain stable as this is the installation and pre-construction measurement stage. Mote 11 in the $y-$direction indicates an upward trend; however, it is skewed by errors in the initial starting point, which is stabilized before work begins. In Phase 2 (8/25/09 to 9/8/09), the $x-$direction for both motes and the $y-$direction for Mote 11 gets closer to level, while the $y-$direction for Mote 8 starts to become level and then becomes more unlevel. The pews are removed as well as the base boards and flooring during this time period. It is possible that the $y-$direction of Mote 8 is affected differently due to its

location on a raised platform behind the altar. As a result, it could be impacted by the removal of the main floor as well as the floor on the platform. Due to the loss of power during Phase 3 (9/8/09 to 9/15/09), it is assumed that the large jump in measurements are due to the digging out of the center span piers. An offset is observed due to changing of the batteries at other times, however, the shift is not uniform and therefore cannot be normalized in this case. The interior joist and beam repair in Phase 4 (9/15/09 to 10/2/09) cause the motes to trend in the level direction. The year 2009 was extremely rainy as indicated in the long rain delay in Phase 5 (10/2/09 to 10/29/09). It should be noted that the data starts and ends at about the same location during this time. It is concluded that the data remains constant during Phase 6 (10/30/09 to 11/2/09) because the structure is being reinforced and therefore, no major changes are occurring. During Phase 7 (11/3/09 to 11/10/09), the church is leveled for the first time. From that point on, the contractor observes it settling out of level due to the soil conditions. The church is jacked up and down at various points from Phase 7 until it is finally set (12/18/09) so movement is seen throughout Phases 7-10 (11/3/09 to 12/18/09). The WSN is removed on 12/19/09. Note that the trend line is level (0°) for all motes when the last measurements are recorded.

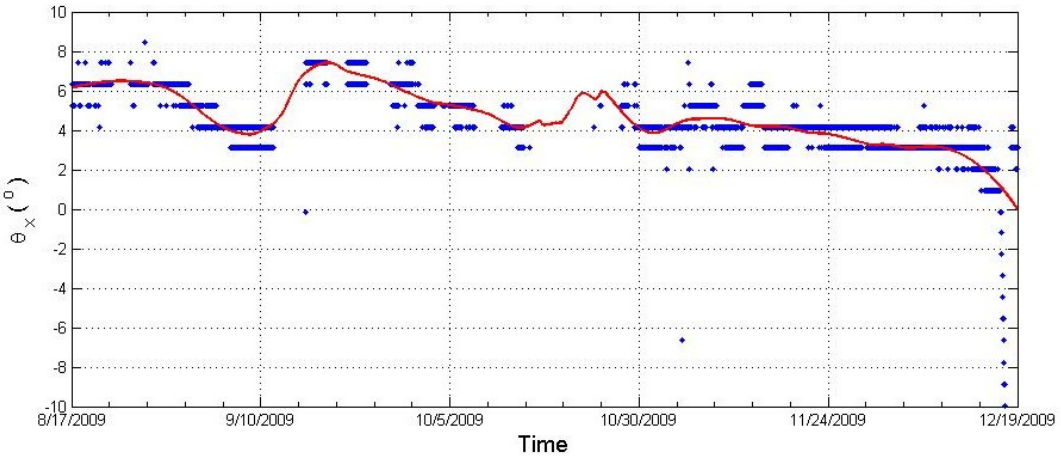

Figure 3-7. Tilt of Mote 8 in $x-$direction

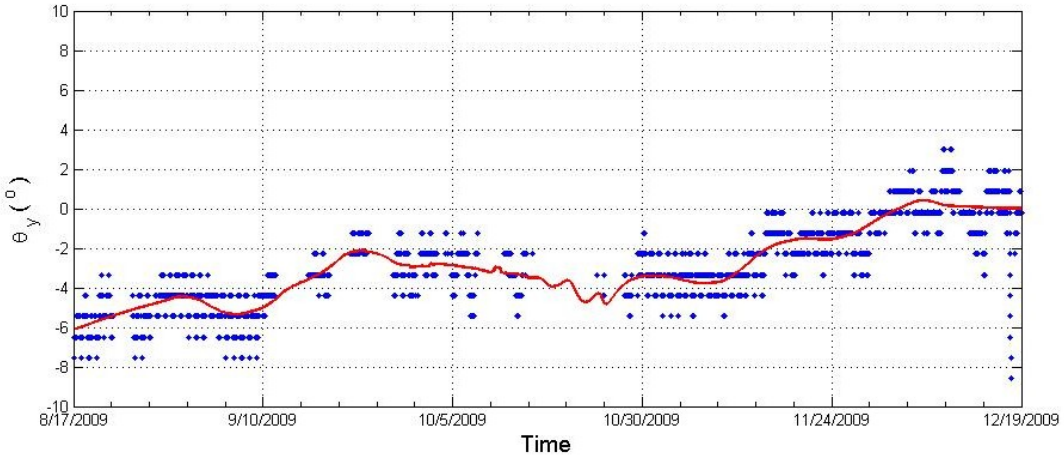

Figure 3-8. Tilt of Mote 8 in $y-$direction

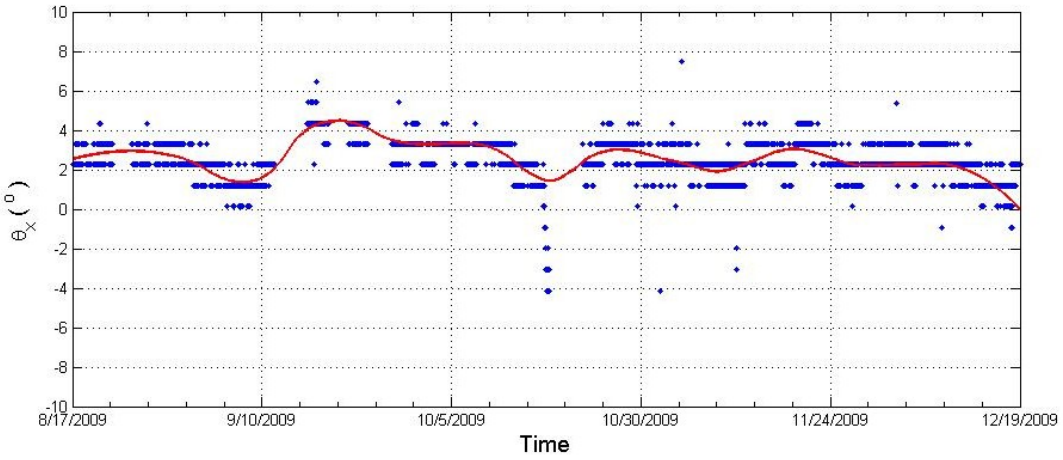

Figure 3-9. Tilt of Mote 11 in $x-$direction

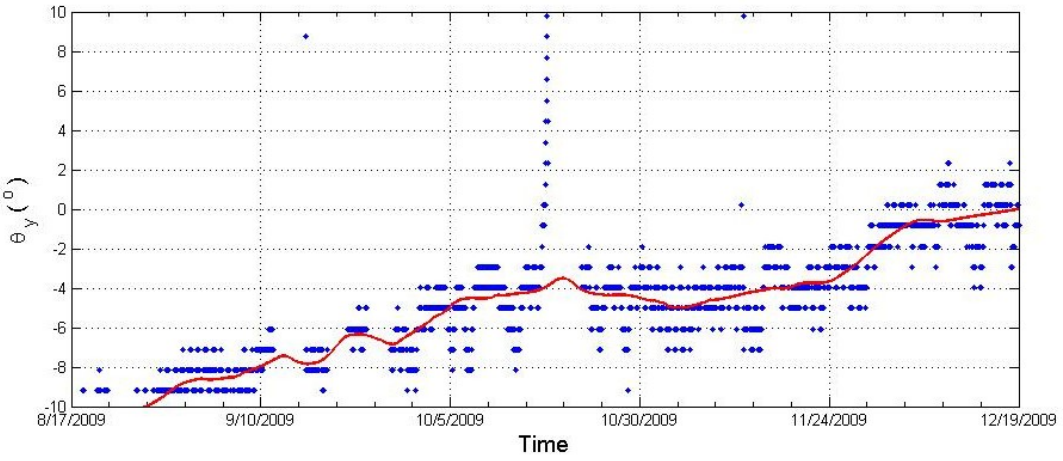

Figure 3-10. Tilt of Mote 11 in $y-$direction

Several issues occur during the installation and data acquisition phases of the project. As previously mentioned, the power source for the motes must be self contained, so research is conducted to find the best batteries for the application. To properly estimate the battery life, motes are programmed for three different time increments (2

seconds, 15 minute, and 1 hour). The voltage of the new batteries is measured and the motes are then turned on at the same time and recorded measurements for three days, at which point the voltage is measured again. This process is used for all three batteries tested: Duracell Alkaline AA, Panasonic Industrial Alkaline AA, and Energizer Lithium AA. From this data, it is estimated that Energizer Lithium AA batteries set at 15 minute increment measurements would produce the optimal battery serviceability because the batteries would only need to be changed once a month. There is little difference in the reduction of battery power between the 15 minute increment and 1 hour increment. Since the 15 minute increment motes provide more data points, they are used. In the field, the batteries last anywhere from 3 days to 1 week longer than expected before losing power.

Due to the location of the church in a region that receives frequent severe thunderstorms, there is a problem with the loss of electricity in the storms and thus turning off the computer that collects the data. To resolve this issue, the computer is connected to an uninterruptable power supply on October 5th. Since its installation, the computer did not lose power during storms.

CHAPTER IV

ST. PAUL LUTHERAN: SERBIN, TEXAS (USA)

St. Paul Lutheran, a historic masonry church with a timber-framed roof (Figures 4-1 & 4-2) in Serbin, Texas, is the focus of the field study. This structure is chosen to investigate the effects of foundation work on the tilt of the walls, which have extreme cracking in some locations. Information on the historic structure is provided as a background, followed by the rehabilitation tasks. The wireless monitoring approach is explained, and then the results are explained.

Historic Structure

This structure, one of the Painted Churches of Texas, was completed in 1871 due to the efforts of Reverend Johan Kilian and a group of approximately 500 Lutheran Wends who emigrated from the region of Kotitz, Germany to escape religious oppression and for the right to speak their Wendish language (Geva 2009; Lammert 2010).

Figure 4-1. Exterior view of St. Paul Lutheran

Figure 4-2. Interior view of St. Paul Lutheran

As was typical of immigrants, the Wends brought parts of their culture with them to America. This is evidenced in the similarities between the Lutheran Church in Kotitz, Germany (Figure 4-3) and St. Paul Lutheran in Serbin, Texas (Figure 4-1). Although they were built approximately 200 years apart, Nielsen (1989) notes that both churches are designed with a "simple folk Gothic style". In addition to a shared architectural style, the churches have a similar floor plan and construction plan. They each have a single nave rectangular plan with a bell tower and walls built of 0.762 m thick stone: sandstone in Germany and red sandstone in Texas. According to construction documents quoted in St. Paul Lutheran (2004), the church was to be "21.34 m long by 12.19 m wide, with walls 7.32 m high". Four clear glass windows were placed on each side along the length

of the church. The original exterior finish was coarse, while the interior had a fine finish. There was to be a tower and steeple, topped by a weathervane, which had a metal ball containing the history of Serbin, as written by Reverend Kilian. In comparison, the Kotitz Church was 17.68 m long by 11.58 m wide with a tower and steeple. A fine finish was used on both the interior and exterior, and the clear glass windows were located predominantly along the length of the structure.

Figure 4-3. Exterior view of Kotitz Church (Geva 2009)

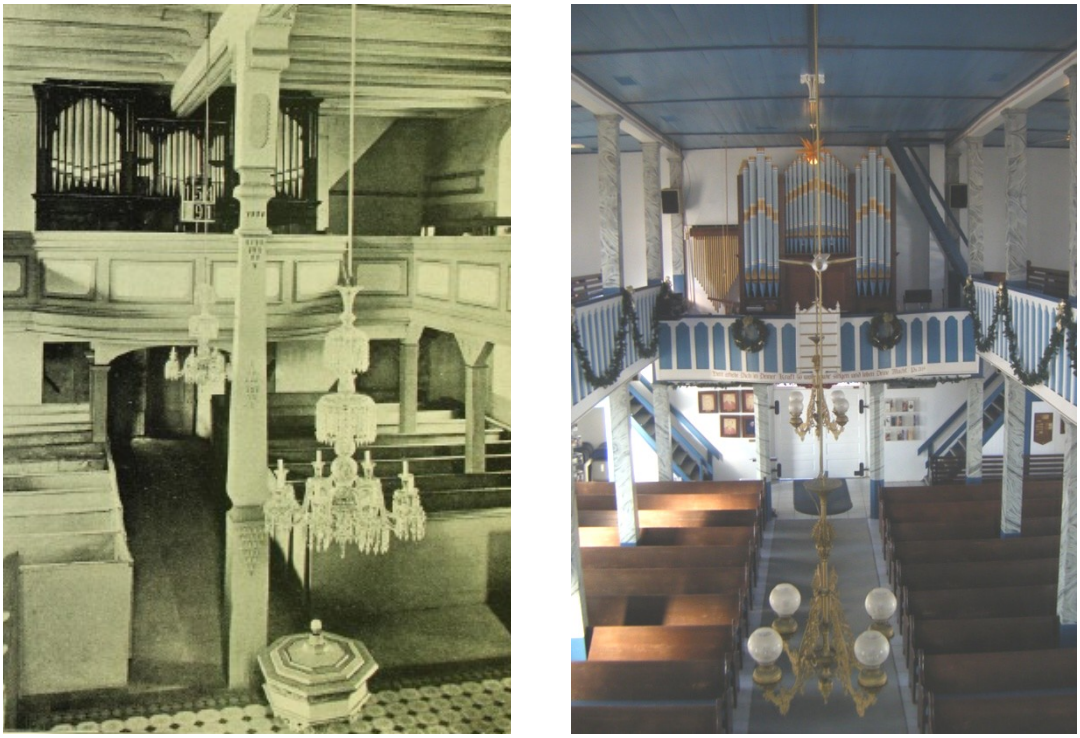

Figure 4-4. Original interior of Kotitz Church (left, Gurlitt 1910) and interior of St. Paul Lutheran (right)

While these structures have similarities on the exterior, the most striking resemblance is found in the interior, where the painted turquoise and blue interior, ornate chandeliers, pipe organ above the entrance, and multi-sided balcony of St. Paul mimic the Kotitz Church (Figure 4-4). In fact, the chandeliers at St. Paul's are the original kerosene lamps that have been converted for electricity (St. Paul 1980). Not only were the physical attributes of the interior similar, but the seating protocol of men sitting in the balcony and women and children staying on the ground floor was strictly followed (St. Paul 2004).

According to Lammert (2010), “St. Paul’s is one of the oldest churches in America in continual use since its construction”. It is also said to have the highest pulpit in Texas because it is set on the balcony level, approximately 6.1 m off the ground floor.

Rehabilitation

Although the 0.762 m thick walls create a robust structure, the church is having settlement issues which are focused primarily towards the front entrance (west) of the church. These problems are most clearly manifested in the extensive cracking in the 1.27 cm thick plaster walls. The front exterior façade has cracking along almost the entire wall, which transferred through the 0.762 m thick stone walls and into the plaster on the interior. The load path of the structure is apparent by the extreme cracking in the pointed arches of the windows, which is worst near the front (west) wall and becomes less and less noticeable towards the back (east) wall. In fact, the stained glass windows nearest the front wall have deflected inwards approximately 7.62 to 10.16 cm, causing the glass to crack. In addition to the windows and plaster cracking, the differential settlements of the church have caused the ceiling to separate from the plaster walls at certain locations along the left (north) and right (south) walls. The settlement in the ceiling is delineated in the extreme slope of the beams supporting the ceiling, which is easily visible to the naked eye. Once the construction workers start digging near the foundations, they discover the root of the settlement problems is a large amount of water trapped under the church’s foundations. To alleviate these problems, the foundations under the exterior walls of the church are underpinned, beam stiffeners are poured along the footings and the floor slab is replaced with a floating slab that is structurally detached from the wall

foundations (Figure 4-5). Water barrier mats are installed at the foundation level to redirect water away from the church to ensure water does not become entrapped under the foundations in the future. After the church is stabilized, the exterior and interior are replastered as needed in four stages, starting with a rough plaster and moving to a smooth finish for the interior and a brushed finish for the exterior, both of which are painted a shade of cream (Figure 4-6). Since the front wall has the worst problems, the entire front exterior wall has to be replastered (Figure 4-7).

Figure 4-5. Foundation excavations and new footing (left, St. Paul Lutheran 2010) and footing with beam stiffener (right, St. Paul Lutheran 2010)

Figure 4-6. Four stages of plaster repair

Figure 4-7. Front entrance partially replastered (St. Paul Lutheran 2010)

During construction, the original stone floor is found under the concrete slab (Figure 4-8). The majority of the stone is able to be salvaged and although it is too uneven according to the Americans with Disabilities Act (ADA) standards to be reset on the interior of the church, it is planned to be reused at the entrance. To create a similar feel as the original floor, stone tiles are set on the new concrete slab (Figure 4-8).

Figure 4-8. Original stone floor (left, St. Paul Lutheran 2010) and new stone floor (right, St. Paul Lutheran 2010)

Monitoring

At St. Paul Lutheran, each mote is mounted either on an angle bracket, which is attached to the wall on the balcony level with masonry screws and stabilized with a 3M removable poster strip. The motes are oriented such that the local $x-$ axis is perpendicular to the wall and the local $y-$axis is parallel with the wall. As depicted in Figure 4-9, the motes are located predominantly on the front (west) end of the structure where the majority of the issues are observed. Note, Mote 8 is attached to the underside

of a beam in the utility closed on the ground floor supporting the balcony, Motes 2, 7 and 13 are installed on the beams in the attic that comprise the ceiling above the balcony level, and the remaining motes are installed on the walls of the balcony level.

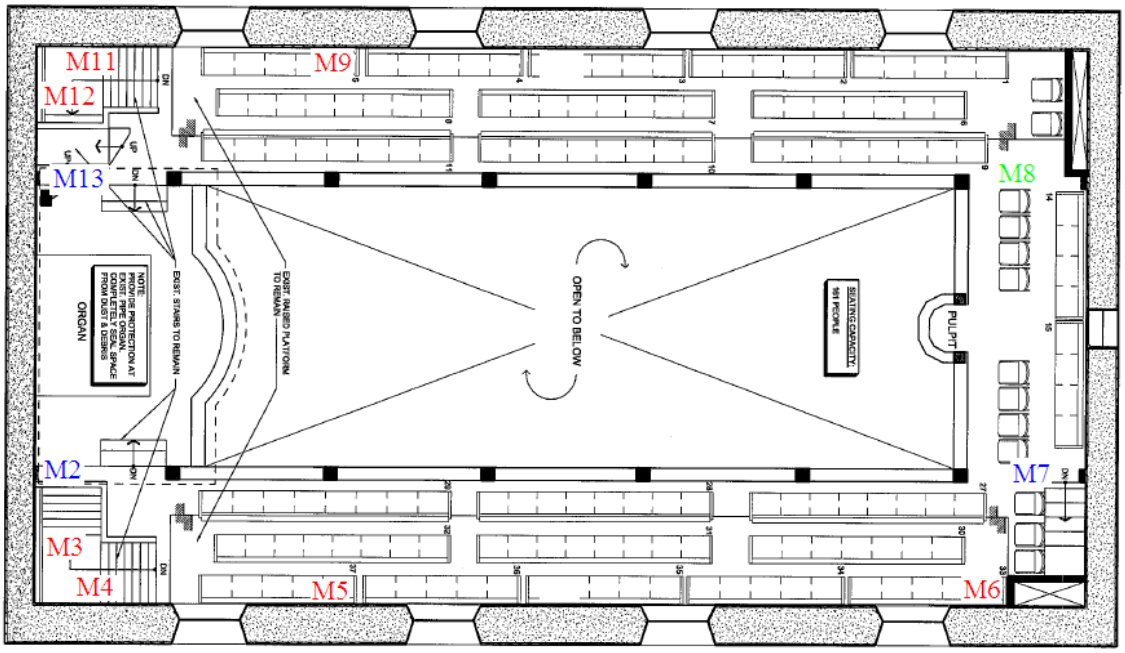

Figure 4-9. Plan view of St. Paul Lutheran with mote placement

The base station and desktop computer are set up along the wall on the balcony level. After all of the motes are in place, the WSN programs are started and data is saved on the computer. Internet access is not possible with the laptop card service provider in this field study due to a lack of coverage in such a remote location. All motes are removed once the structural foundation work is complete.

Results

The WSN is installed three days prior to the start of construction and remains until all structural foundation work is finished and only tasks that would not impact the structure remain. The sensors used in this application have a sensitivity of approximately one degree. They are able to record movements throughout construction as a result of underpinning the foundations and digging under the church.

Motes 2 and 11 are chosen as examples (Figure 4-10). They display the results for a mote installed on an attic floor beam and a mote on the north wall near the stairs, respectively.

Figure 4-10. Mote 2 (left) and Mote 11 (right)

To verify the hypothesized correlation between construction activity and tilt in the walls, the plotted results are compared with the construction schedule. Table 4-1 displays the major activities of construction.

Table 4-1. Construction schedule at St. Paul Lutheran

Start Date	End Date	Description
1/4/10	1/6/10	WSN installed before start of construction
1/7/10	1/12/10	Start excavation and place rebar (south side)
1/13/10	1/14/10	Start pouring around foundations; continue excavation and placing rebar (south side)
1/15/10	1/18/10	Rain delay
1/19/10	1/20/10	Continue excavation and pouring concrete around foundations; start pouring stiffener beams on top of footings (south side)
1/21/10	1/24/10	Clean up for wedding
1/25/10	1/25/10	Remove pews from church
1/26/10	1/26/10	Start excavation and place rebar (north side)
1/27/10	1/27/10	Start pouring concrete around foundations and stiffener beams on top of footings (north side)
1/28/10	2/8/10	Rain delay
2/9/10	2/15/10	Continue excavation, pouring concrete around foundations and stiffener beams on top of footings (north and east side)
2/16/10	2/17/10	Dig hole under church and prepare for more concrete footings; pour footings on east side, including beam under church
2/18/10	2/21/10	Continue pouring footings and prepare for stiffener beam on east side; north side completed; prep west side for excavations
2/22/10	2/22/10	Start excavation and place rebar (west side)
2/23/10	2/23/10	Snow delay
2/24/10	3/4/10	Start pouring around foundations; continue excavation and placing rebar (west side); start removing plaster from exterior walls
3/4/10	3/10/10	Foundation work complete; demo existing concrete slab, remove original stone floor underneath; Remove WSN on 3/10/10

As was the case in the previous field study, the $y-$direction indicated more movement than the $x-$direction throughout the monitoring process. The first few days (1/4/10 to 1/6/10) do not display any movement because construction does not start until 1/7/10. At the start of construction and as excavation and pouring concrete around the foundations commence (1/7/10 to 1/14/10) all motes trend out of alignment initially but then turn back towards the level position. This seems to indicate shifts in the walls

during excavation which are recovered once the concrete is poured. From 1/15/10 to 1/18/10, construction is impeded due to a rain delay. During this time, each mote continued to level out. It is presumed that this occurred as the concrete gained strength and increased the stability of the structures foundations which are excavated. After the rain delay, the contractor has a couple of days (1/19/10 and 1/20/10) to continue work on the foundations before stopping work again to clean up for a wedding (1/21/10 to 1/24/10). The measurements are fairly stable during this cleaning period. The next construction activities are to continue excavation and pouring concrete around the foundations and stiffener beams on top of the footings (1/25/10 to 1/27/10). In this short time, little movement is detected by the motes. However, Mote 11 did become more level in the $y-$direction. Another rain delay disrupts construction from 1/28/10 to 2/8/10. Mote 11 has less movement in the second half of construction due to its location on the stone wall rather than on a wooden beam supporting the ceiling. This indicates that as the concrete is poured and cures, it stabilizes the structure so that Mote 11 sees less and less movement. The WSN is removed on 3/10/10. As can be seen, the trend line is level (0°) for all motes when the last measurements are recorded. Overall, Mote 2 detected more movement than Mote 11. This is because Mote 2 is installed on a wood beam in the attic whereas Mote 11 is attached to the stone wall. Obviously, stone is much more rigid than wood so more could be detected. All of the motes become less level during the rain delay. It should be noted, however, that this shift is fairly small (typically one degree or less). As construction began again (2/9/10 to 2/22/10) and they continue excavation and pouring concrete around the foundations, Mote 2 becomes more

level while Mote 11 remains relatively unchanged. Since it only lasts one day, the structure does not have any significant movement during the unheard of snow delay (2/23/10). After the snow delay, the only remaining foundation work is to finish excavation and pouring concrete around the foundations (2/24/10 to 3/3/10). At this point, the majority of the structure is secured, as evidenced by the relatively small amount of movement (if any) recorded by the motes, excluding Mote 2 in the $y-$ direction. The foundation work is completed on 3/4/10 and as can be seen, the motes remain fairly stable after this point, except for Mote 2 in the $y-$direction. It is unclear as to what caused this shift while everything else remained unchanged, but as previously stated, this mote is on a wooden beam and is therefore more susceptible to movement. The fact that the motes (excluding Mote 2 in the $y-$direction) show no significant movement from the end of the foundation work to the end of the measurement period (3/4/10 to 3/10/10) confirms the analysis of the structural engineer that the floor slab is detached from the structural system of the walls. This is proven because during this time, the existing concrete slab is demolished and the original stone floor underneath is removed. Figures 4-11 through 4-14 display the output plots, which are correlated to the construction activities detailed above.

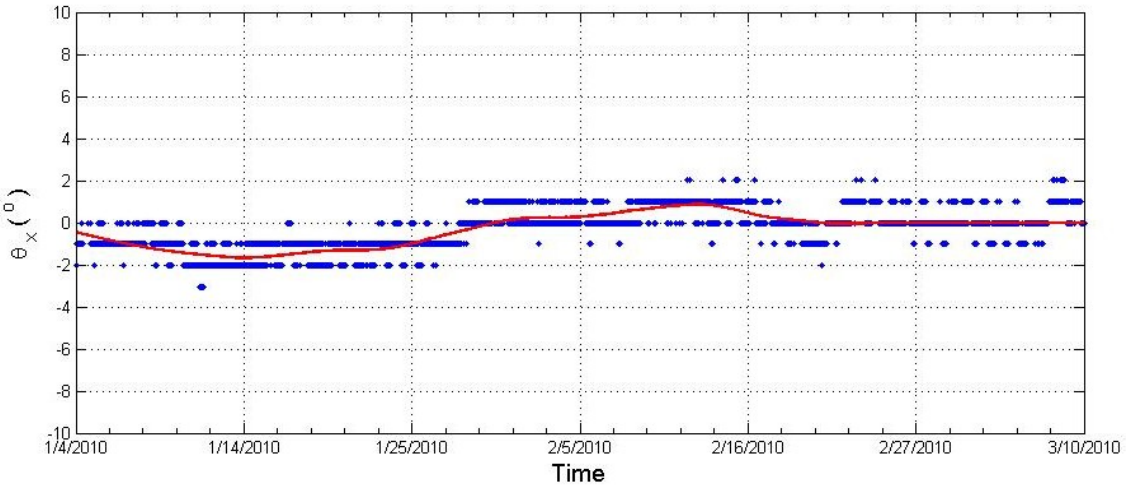

Figure 4-11. Tilt of Mote 2 in $x-$direction

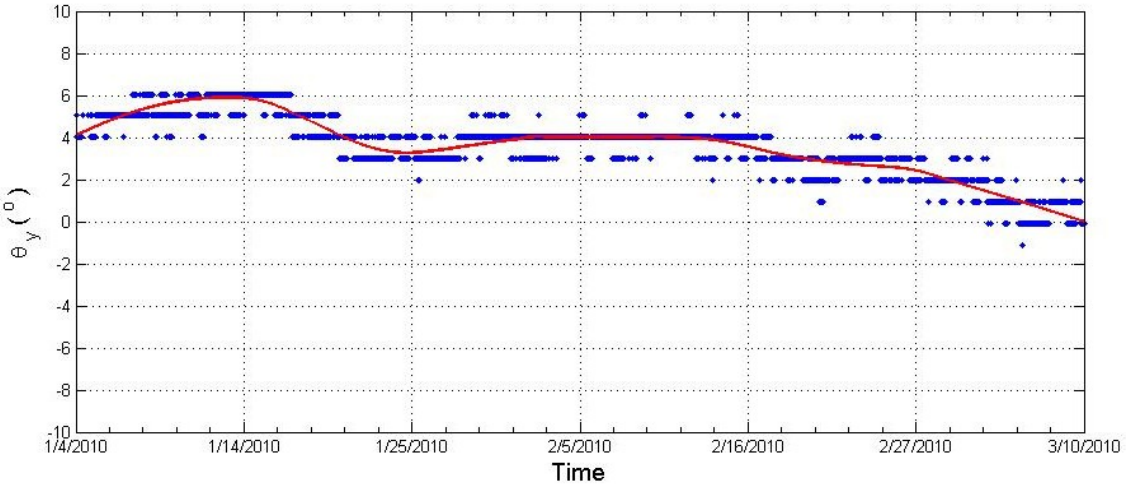

Figure 4-12. Tilt of Mote 2 in $y-$direction

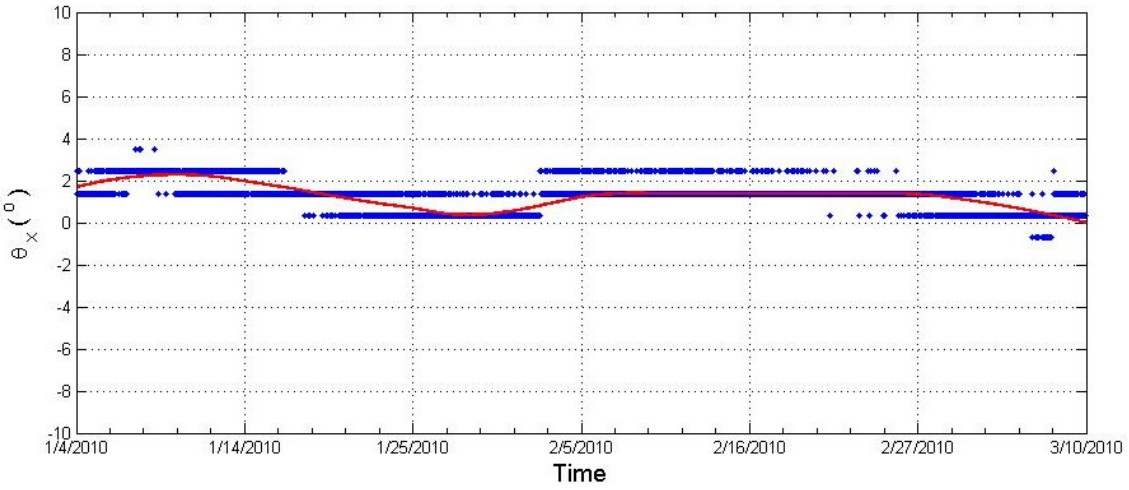

Figure 4-13. Tilt of Mote 11 in $x-$direction

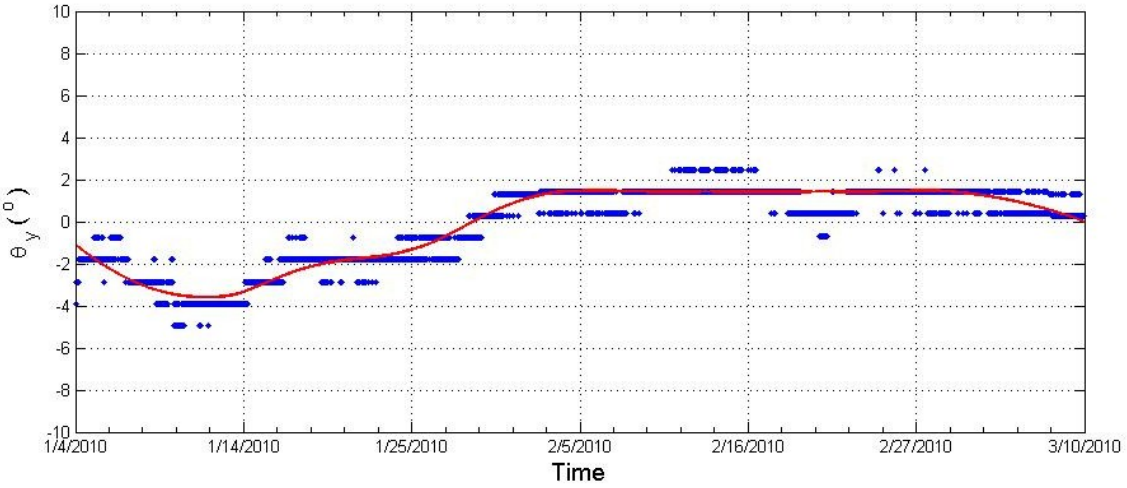

Figure 4-14. Tilt of Mote 11 in $y-$direction

For an additional comparison, the temperature at the church is plotted each day at 20 minute increments (Figure 4-15). This displays the wide range of temperatures for which the sensors can be implemented (Weather Underground 2009).

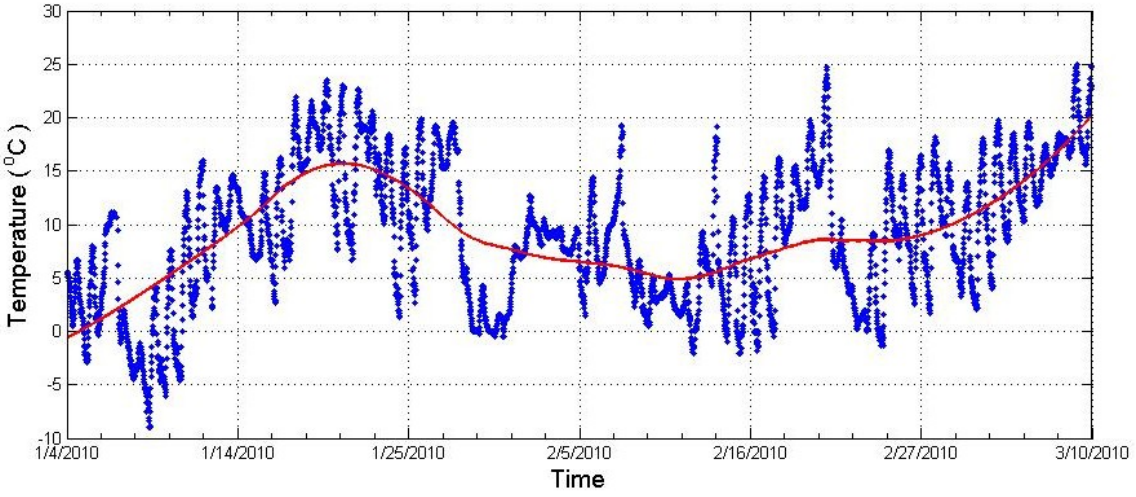

Figure 4-15. Temperature at St. Paul Lutheran during monitoring

Maintaining power and minimizing data loss is the primary limiting factor of the WSN. To address these challenges, the computer and base station are connected to an uninterruptable power supply. For this application, it is determined that batteries are the best power source for the wireless motes. Lab tests are conducted to identify the ideal type of battery and time increment for measurements. In these tests, motes are programmed for three different time increments (2 seconds, 15 minute, and 1 hour). Voltages of the new batteries are measured before installation and take measurements for three days, when the total voltage is measured again. Duracell Alkaline AA, Panasonic Industrial Alkaline AA and Energizer Lithium AA are each tested using each of the time increments. The results concluded that Energizer Lithium AA batteries perform best when the motes take readings at 15 minute increments. Using this configuration, the motes require a change of batteries once a month. As can be seen in

Figures 4-11 through 4-14, these changes greatly improved the consistency of data transmission.

CHAPTER V

JOHANNISKIRCHE: SCHWÄBISCH GMÜND (GERMANY)

The Johanniskirche in Schwäbisch Gmünd, Germany is the structure monitored in this field study (Figure 5-1). The primary issue at the Johanniskirche is not the foundation, but condensation. Therefore, the purpose is to measure climate in the Johanniskirche and develop a condensation risk analysis tool. The history of the structure and rehabilitation approaches are provided, followed by information on monitoring, the analysis software, and the results.

Historic Structure

Construction of the Johanniskirche began around 1220 to 1250 on the foundations of a previous church from the 12th Century. It is a typical late Romanesque column basilica with vibrant sculptural decoration depicting scenes from the animal and fable world as well as plant life. The Gothic and Baroque periods brought about changes to the structure, as it was typical to renovate in the current style with each successive bishop; however, the choir was reconstructed in the 19th Century to reflect its original state through a "Re-Romanization". During this time, Karl Dehner from Rottenburg painted the murals on the walls of the nave that are still there today (Figure 5-2). Although it began as a Roman Catholic Church, it is now used predominantly as a museum and to host special events. The side aisles of the Johanniskirche house original sculpture fragments from the Johanniskirche as well as Heilig Kreuz Münster (Holy Cross Minster Cathedral). The church was constructed with walls of local sandstone (with rubble

infill), a timber plank ceiling and a wood-framed roof with tile shingles. It should be noted, however, that the structure is not water or air tight and allows a constant flow of air from the exterior to the interior and vice versa.

Figure 5-1. The Johanniskirche in Schwäbisch Gmünd

Figure 5-2. Murals on walls of the Johanniskirche (Krüger 2010)

Rehabilitation

Heritage conservation of the Johanniskirche has been underway since 2009 to address the many problems facing this structure. The most critical issues involve the murals on the walls and effects of the interior and exterior climate conditions. Figure 5-3 provides a detailed view of the damage in both the upper and lower levels. Conservationists noticed delamination and deformation of the paint layer in the gilded areas. Paint and pigment loss due to degradation of the binder material as well as paint particles falling off or being washed away by condensation and dust deposition are major points of concern. In addition, the structure has no heating system and therefore the indoor climate can become very humid. This leads to condensation and traces of water running down the clerestory windows, which causes debonding of the mortar joints and material loss. The durability of the sandstone walls is also in question because damaging salts are found in the lower areas of the walls. Figure 5-3 documents the paint and salt damage observed in the structure.

Figure 5-3. Detailed view of damage: paint deterioration in upper level and salt damage in lower walls (Krüger et al. 2010)

To address these issues, loose dust deposits are being removed and water-insoluble binding is applied through Japanese paper (to be removed later). The cracks are remedied with the use of a special lime mortar, and temperature monitoring of the Johanniskirche hopes to improve the treatment of the climate problems.

With respect to moisture migration problems, the primary concern is that any solution should not interfere with the original aesthetic appearance of the cultural heritage site. An initial proposed solution is to use 24 cm thick thermal insulation and permeable sheeting on the floor of the intermediate ceiling. While this approach should theoretically reduce humidity inside the structure and increase room temperature, it cannot be confidently assumed that the humidity will be adequately reduced at all times. In addition, this approach only affects the humidity and temperature and does nothing to

minimize the effects of the cold walls and windows. To account for temperature, humidity and the cold walls and windows, three possibilities are presented (Krüger et al. 2010):

- Installation of a dehumidifier and/or heating system
- Installation of electrical ventilation system in intermediate ceiling
- Use of natural ventilation by opening doors and windows as well as structural modifications to influence the natural air exchange rate during critical conditions.

Monitoring

The SmartMote WSN implemented at the Johanniskirche is developed and improved as a part of the European Union SMooHS (Smart Monitoring of Historic Structures) Project (2008). According to the project website (www.smoohs.eu), the primary goals of SMooHS are (SMooHS: Smart Monitoring of Historic Structures 2010):

- Creation of smart monitoring systems utilizing small sensors which adhere to the stringent requirements imposed on historic structures to monitor key features, in an effort to improve preservation of cultural heritage structures
- Smart data processing with built in material deterioration models to evaluate threats, warn building supervisors and suggest appropriate methods to minimize damage
- Creation of user-friendly, modular open source software with the possibility of continuous updates and improvements.

For monitoring at the Johanniskirche, motes equipped with SHT15 sensor boards are placed at ten locations throughout the structure. At five of these locations, an

additional sensor is installed on the exterior and connected to the interior mote with a wire through a small hole near the window or between planks in the ceiling. Figure 5-4 displays a mote installed in the interior of the church. The locations of the motes are detailed in Figures 5-5 through 5-7.

Figure 5-4. Wireless sensor installed in the Johanniskirche (SmartMote 2010)

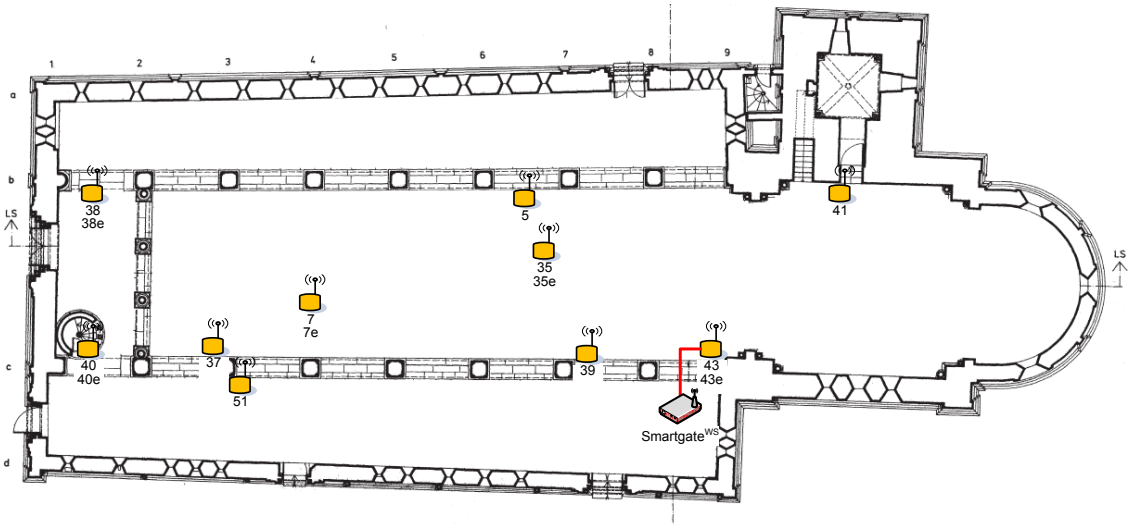

Figure 5-5. Plan view of mote placement at the Johanniskirche (Krüger et al. 2010)

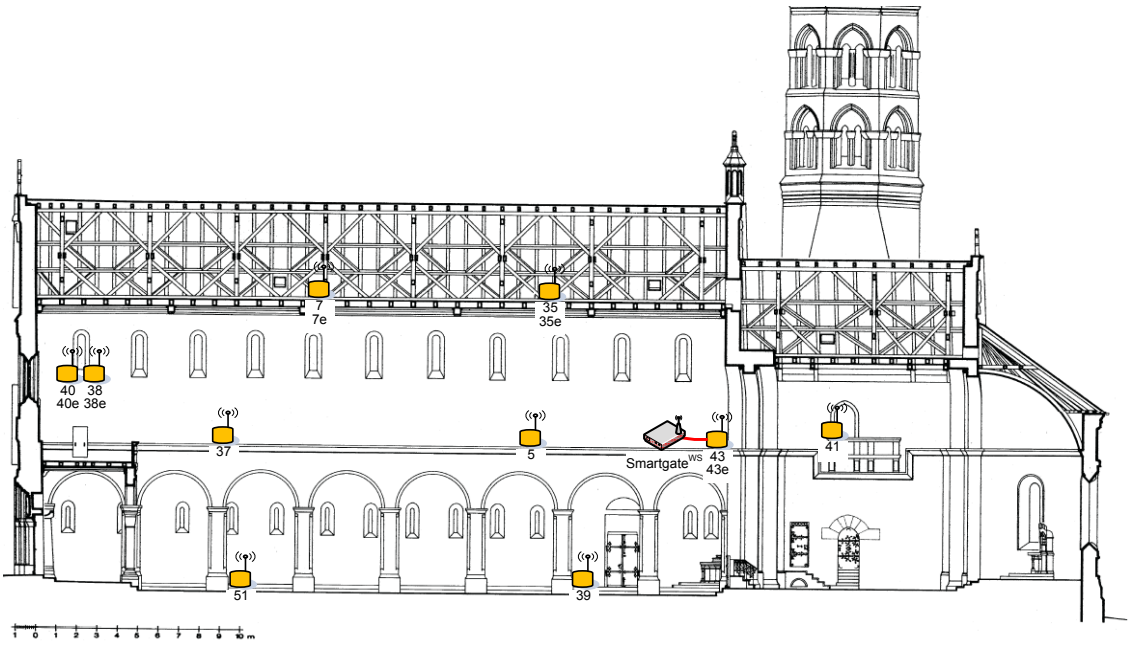

Figure 5-6. Longitudinal section of mote placement at the Johanniskirche (Krüger et al. 2010)

Figure 5-7. Cross-section of mote placement at the Johanniskirche (Krüger et al. 2010)

Once the motes are installed, they wirelessly transmit the collected data to the base station (Smartgate^{WS}). The Smartgate^{WS} sends the data to a SQL database via the internet, where the data can be further analyzed. As a part of this analysis, real-time data can be viewed online (www.smartmote.de/Johanniskirche/Johanniskirche.html). Through the online portal, one can view the data as a table, diagram or compare two motes in graphical format for a user-defined time span. As can be seen in the diagram format (Figure 5-8), the node is identified and color coded based on the current condition: blue indicates acceptable temperature and relative humidity values, while red humidity number indicates risky conditions such as 100% humidity. If the mote ID, temperature and humidity are all orange, it indicates the base station has not received data from that mote in at least 15 minutes and the same situation for red values indicates data transmission interruption of at least 30 minutes. The WSN used to collect climate data at the Johanniskirche is developed by Krüger et al. (2010) and has a radio frequency transmission reliability of 99% within a 15 minute time period after detection of critical ambient moisture inside the church.

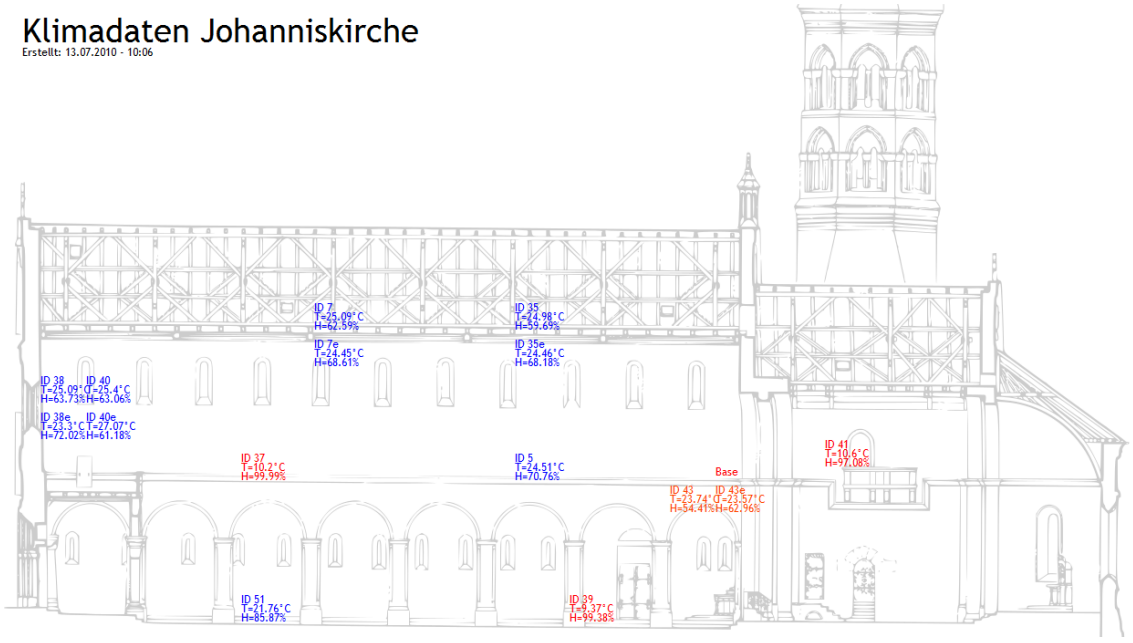

Figure 5-8. Online diagram of the Johanniskirche with real-time data (SmartMote 2010)

WUFI®

WUFI® (Wärme und Feuchte instationär, or Heat and Transient Humidity), a software program which incorporates the newest research in liquid transport and vapor diffusion in construction materials to track the flow of moisture through a building cross-section, is used for the climate impact analysis of the Johanniskirche. The user has the option to use predefined material properties or to input the minimum requirements of: bulk density (kg/m³), porosity (m³/m³), specific heat capacity (J/kg K), dry heat conductivity (W/mK) and dry diffusion resistance factor (-) to specify their own material. Climate data can also be assumed from test reference years (TRYs) or user defined. If neglecting the effects of solar irradiance and counter radiation, the minimum user defined inputs for climate files are temperature and relative humidity. For this application, user-defined

material properties are used for the layers and the climate data measured with the WSN is formatted for use as exterior and interior climate files. The program has several options for output formats including a film (Figure 5-9) of user defined time increments (typically one hour) which plots temperature, relative humidity and moisture content through the material cross-section, and output plots for total water content, water content by layer, temperature, relative humidity, and dew point, all of which can be separated into interior and exterior conditions. The time step film is especially helpful for visualization of moisture flow through the material cross-section. It displays both the conditions at the end of the analysis, indicated by a darker line, as well as the envelope of the entire time span analyzed, depicted as a shaded area. As seen in Figure 5-9, red denotes temperature (°C), green symbolizes relative humidity (%) and blue indicates water content (kg/m³).

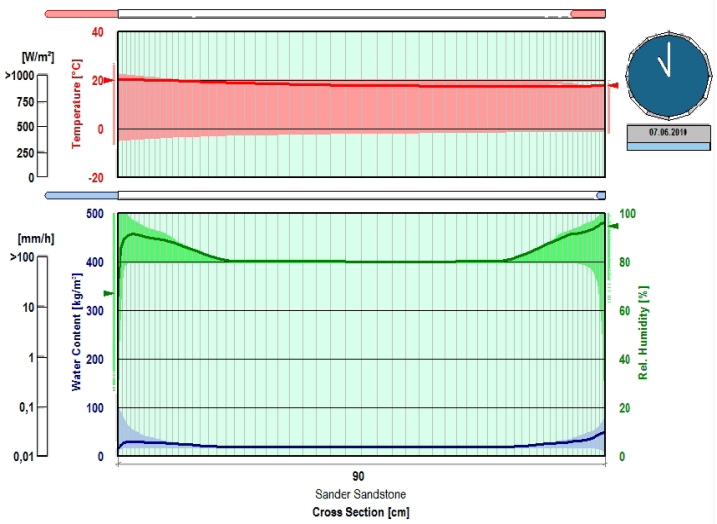

Figure 5-9. Time step video screenshot from WUFI® for exterior (left side, Mote 38e) and interior (right side, Mote 5) surfaces

Results

Data is continuously collected from the WSN since installation in the Johanniskirche on 12/22/09. This data is simulated in WUFI® and those results are used as the basis for the risk analysis criteria.

The process begins with continuous climate data input of air temperature (°C) and relative humidity (%) from the wireless sensor network employed at the Johanniskirche. From these inputs, the dew point (°C) and absolute humidity (g/m^3) are calculated for the interior and exterior (Sensirion 2009)

$$\vartheta_{i,e,dew}(t) = 243.12\left(\frac{\ln\left(\frac{RH_{i,e}}{100}\right)+\frac{17.62\times\vartheta_{i,e}(t)}{243.12+\vartheta_{i,e}(t)}}{17.62-\left[\ln\left(\frac{RH_{i,e}}{100}\right)+\frac{17.62\times\vartheta_{i,e}(t)}{243.12+\vartheta_{i,e}(t)}\right]}\right) \tag{5.1}$$

$$d_{i,e,v} = 216.7\left(\frac{\frac{RH_{i,e}}{100}\times 6.112\times e^{\left(\frac{17.62\times\vartheta_{i,e}(t)}{243.12+\vartheta_{i,e}(t)}\right)}}{273.15+\vartheta_{i,e}(t)}\right) \tag{5.2}$$

where $\vartheta_{i,e,dew}(t)$ = interior/exterior dew point temperature (°C), $\vartheta_{i,e}(t)$ = measured interior/exterior temperature data (°C), $RH_{i,e}$ = measured interior/exterior relative humidity (%), and $d_{i,e,v}$ = interior/exterior absolute humidity (g/m³).

This leads to the first data analysis point in the process. At this point, the exterior dew point is compared with the minimum temperature of all interior motes. If $\vartheta_{e,dew}(t) > \min(\vartheta_i(t))$, there is a great risk of condensation, so the program will indicate

(with a red light in future development) that the building manager should minimize door and window opening. Otherwise, the data will be averaged over a 15 minute time span and the exterior dew point, $\vartheta_{e,dew}(\Delta t = 15)$, and the minimum of all interior motes, $\min(\vartheta_i(\Delta t = 15))$, will be calculated for the next decision making step. This data is used in the condensation risk analysis, where a temperature correction factor, α, is introduced, which is currently estimated as $\alpha = 1°C$. Future application of this criteria will help optimize the α value. The program will again indicate that door and window opening should be minimized if $\vartheta_{e,dew}(\Delta t) > \min(\vartheta_i(\Delta t)) - \alpha$. If not, the evaporation reliability is calculated (Sensirion 2009)

$$P_{evap} = 1 - \frac{e_e}{e_{w,e}} \tag{5.3}$$

$$e_{w,e} = 6.112 \times e^{\left(\frac{17.62 \times \vartheta_{i,e}(t)}{243.12 + \vartheta_{i,e}(t)}\right)} \tag{5.4}$$

$$e_e = \frac{RH_e \times e_{w,e}}{100} \tag{5.5}$$

where P_{evap} = evaporation reliability, $e_{w,e}$ = exterior saturation vapor pressure (hPa), e_e = exterior vapor pressure (hPa), $\vartheta_{i,e}(t)$ i,e = measured interior/exterior temperature data (°C), and RH_e = measured exterior relative humidity (%).

The evaporation reliability correction factor, β, is introduced for the next decision, where β is currently estimated as 0.5. Further development will refine the

estimate of the β value. If $P_{evap} < \beta$, the program will indicate the need to minimize door and window openings. Otherwise, it will continue to the final decision point, which checks for frost risk using the criteria $\min(\vartheta_i(t)) < 0°C$. A frost risk exists if the inequality is true and the system will indicate the need to control door and window opening (with a yellow light in future development). Otherwise, the building manager can increase the air exchange rate (a green light in future development).

Once the decision is made to (i) minimize door and window opening, (ii) control door and window opening or (iii) increase air exchange rate, a condensation estimate (g/m^3) is calculated by

$$C = d_{e,v} - d_{i,v} \tag{5.6}$$

where C = condensation estimate, $d_{e,v}$ = exterior absolute humidity (g/m^3), and $d_{i,v}$ = interior absolute humidity (g/m^3).

The overall user output is in the form of a plot vs. time (in hours or days) with the interior and exterior dew point (°C) on the left axis and the condensation estimate (g/m^3) on the right axis. Figure 5-10 displays the developed risk criteria protocol detailed above.

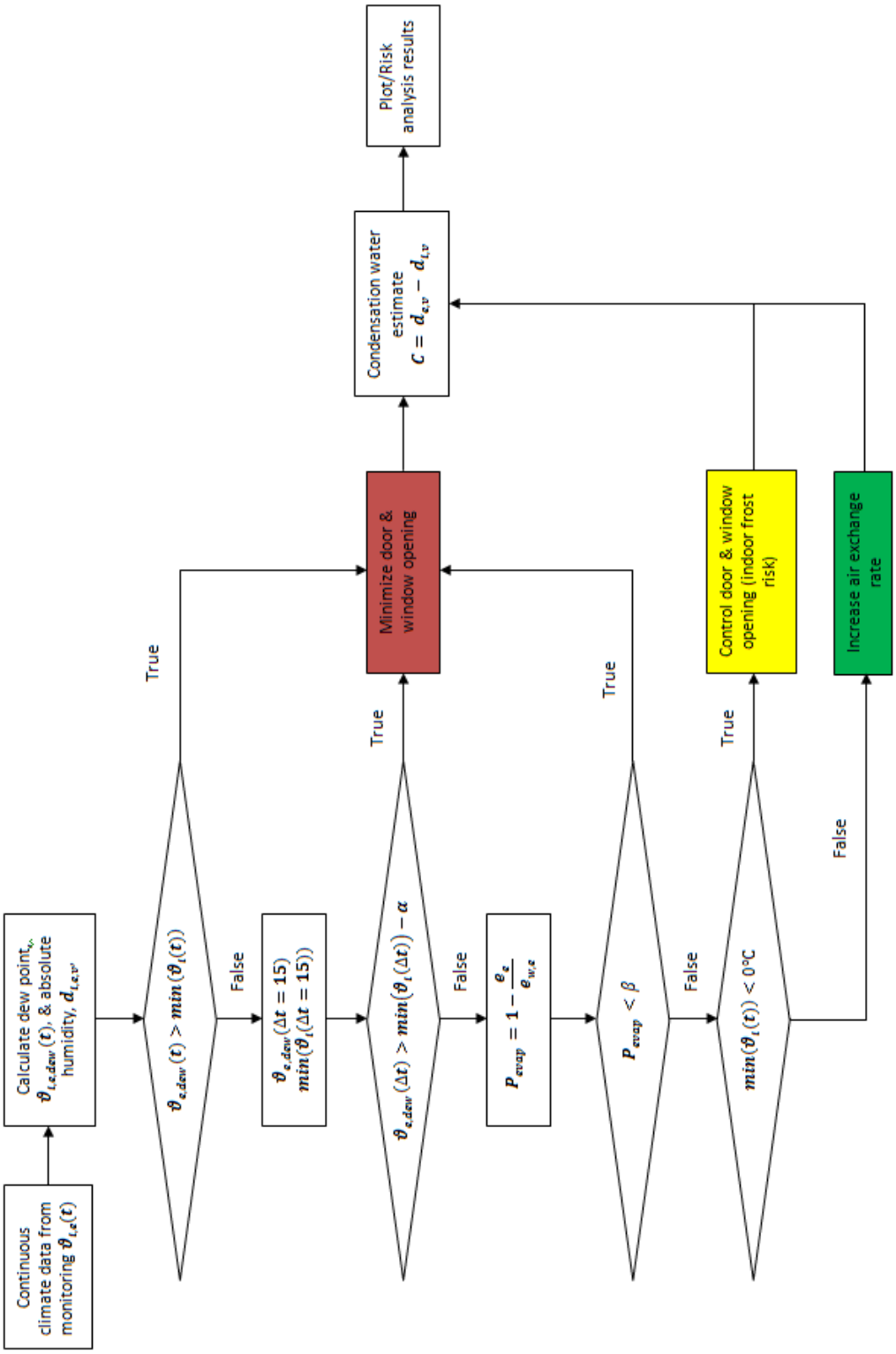

Figure 5-10. Moisture migration risk analysis flow chart

Figure 5-11 is an example of output from the risk analysis criteria using interior dew point (Mote 5), exterior dew point (Mote 38e) and the calculated condensation estimate. As seen in the Figure 5-11, condensation occurs when the exterior dew point is above the interior dew point, and likewise, evaporation occurs when the interior dew point is above the exterior dew point. Note, specifically, that the condensation estimate is a good indicator because condensation was observed at the Johanniskirche on 2/26/10 and the plot indicates condensation.

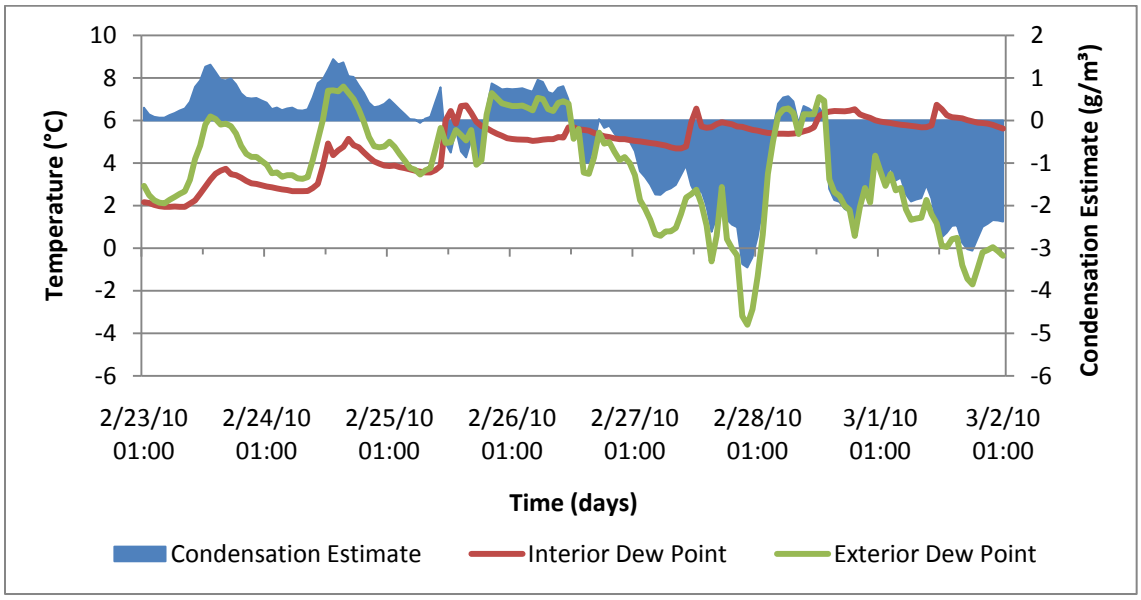

Figure 5-11. Week 10 interior dew point, exterior dew point and condensation estimate over time

To better understand the process, a plot of the measured and calculated data relationship for interior conditions (Mote 51) and exterior conditions (Mote 38e) are separated by elevation in the structure. Figure 5-12 depicts the levels that are compared

and Figures 5-13 through 5-17 display the plots for each of the five levels from 5/25/10 to 5/28/10. This time span is selected because condensation is documented on the floor of the church on 5/26/10. These plots provide valuable insight into locating areas of critical climate conditions. The ground level (Figure 5-13) has the highest condensation estimate during the condensation event of approximately 1.69 g/m³. At mid height (Figure 5-14), this value is almost cut in half at approximately 0.89 g/m³. In the clerestory (Figure 5-15), the condensation is again cut in half with a value of approximately 0.43 g/m³. Even higher, at the intermediate ceiling (Figure 5-16), the condensation estimate again decreases to approximately 0.32 g/m³. However, this trend ends at the attic level (Figure 5-17), which records the second highest condensation estimate of approximately 0.99 g/m³. This confirms the initial hypothesis that some of the moisture in the structure entered through the roof.

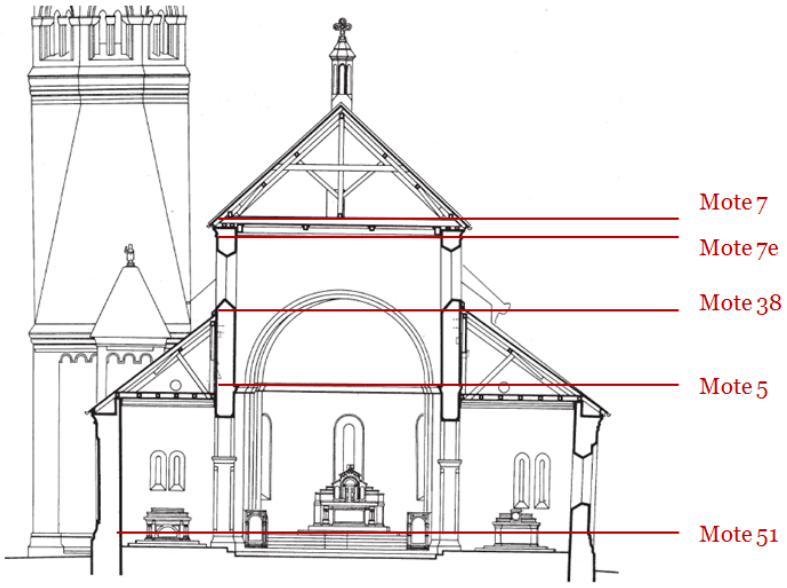

Figure 5-12. Mote elevation on the Johanniskirche cross-section

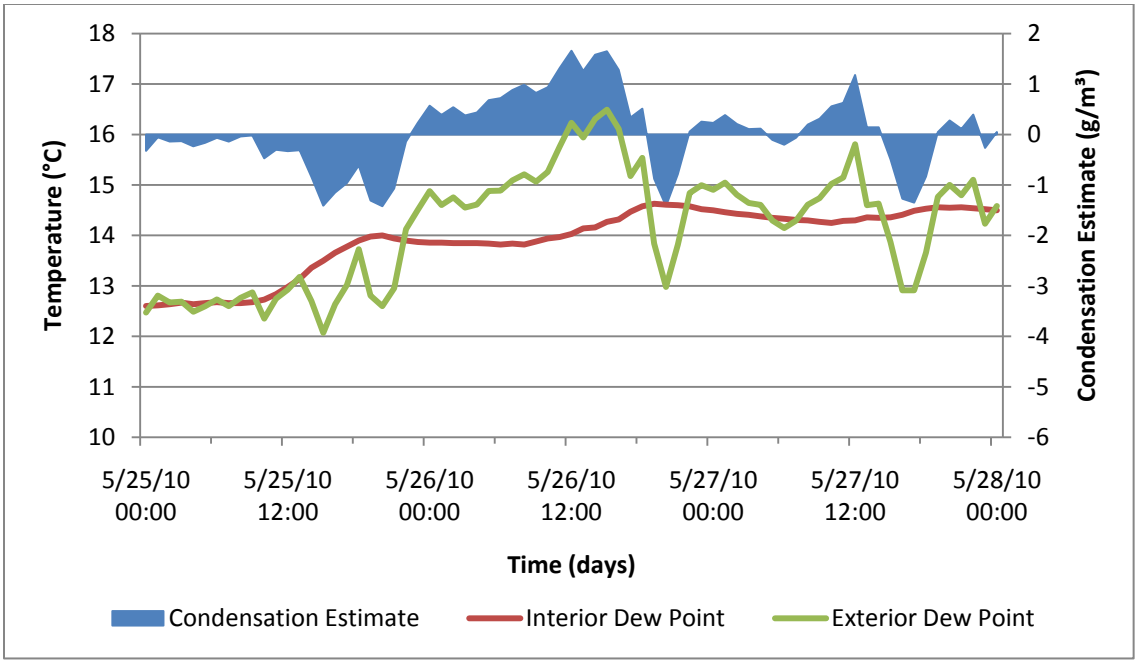

Figure 5-13. Measured and calculated data relationship at ground level (Mote 51)

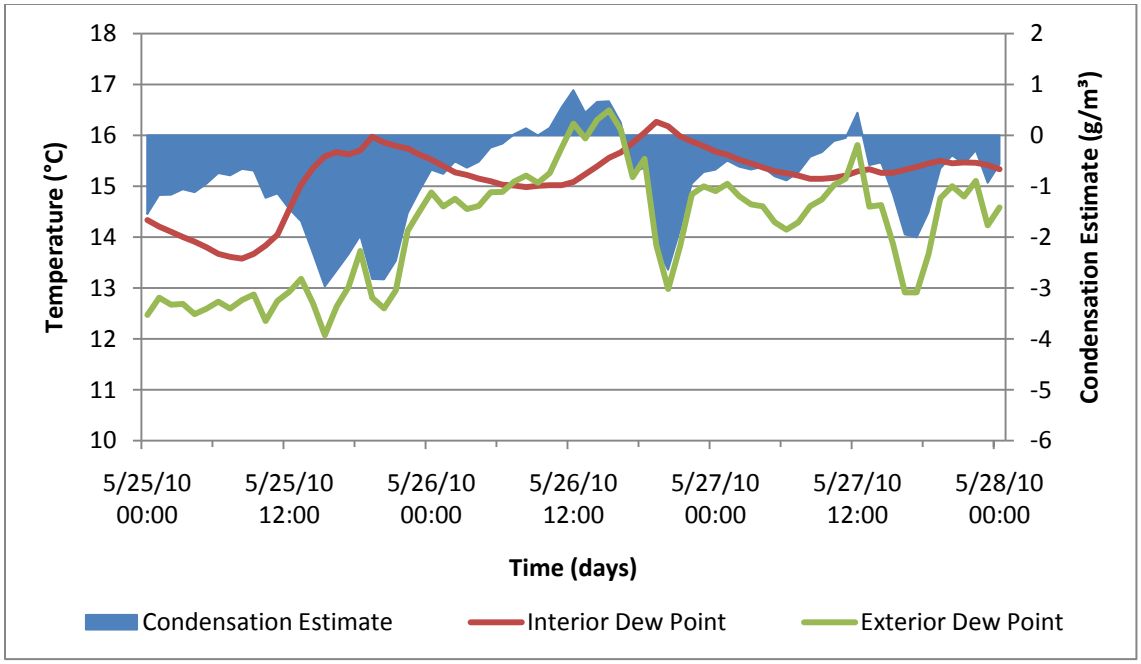

Figure 5-14. Measured and calculated data relationship at mid height (Mote 5)

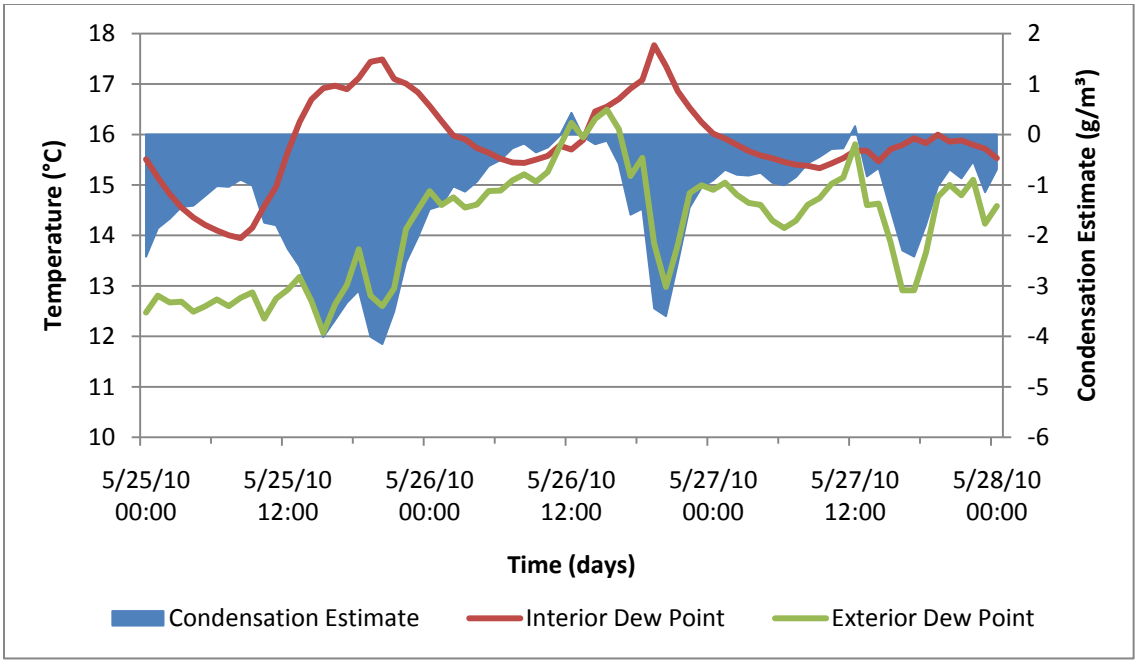

Figure 5-15. Measured and calculated data relationship at clerestory (Mote 38)

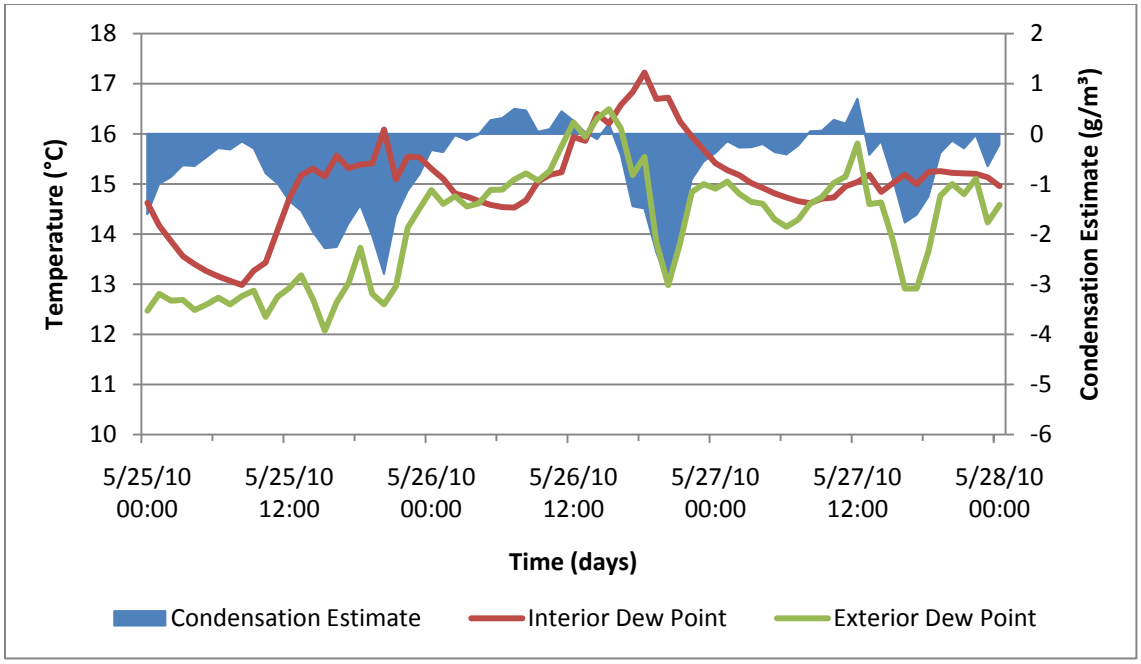

Figure 5-16. Measured and calculated data relationship at intermediate ceiling (Mote 7e)

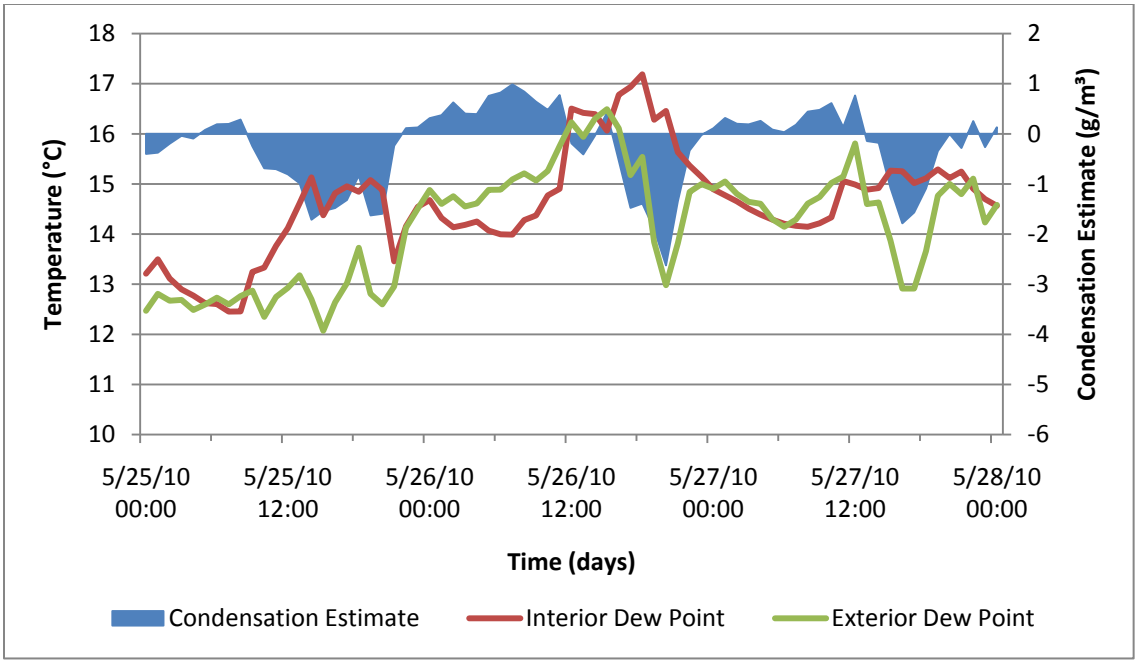

Figure 5-17. Measured and calculated data relationship at attic level (Mote 7)

Figure 5-18 displays the percent of time per week at which WUFI® output has a correlation larger than 0.8 with the calculated condensation estimate from the measured data over time in weeks. Note that in this correlation calculation, negatively correlated data is excluded. The two data points which fall below 70% are insignificant because they represent weeks where data is missing and therefore, the values calculated are based solely on linear interpolation between collected data. Future optimization of the temperature correction and evaporation reliability correction factors will improve the correlation between the WUFI® data and the condensation estimate.

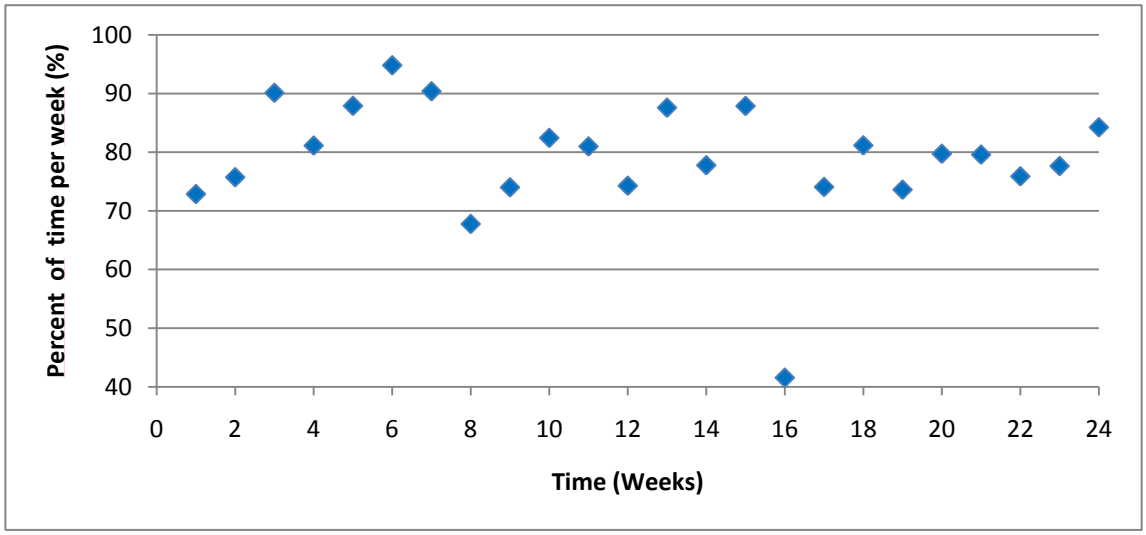

Figure 5-18. Percent of time per week at which WUFI® output has a correlation larger than 0.8 with the calculated condensation estimate from measured data vs. time (excluding negatively correlated data)

Future endeavors will serve to further improve this condensation risk assessment tool. Field implementation will provide more information to optimize the variables α and β. Suggested improvements to the output, such as color coded lights for specified actions will advance the interface with the user. Additionally, the incorporation of short term forecasts in condensation risk prediction can minimize adverse effects on the structure.

CHAPTER VI

CONCLUSIONS

Inspired by the incidents at the Virginia State Capitol and the Texas State Capitol mentioned in the introduction, the long term goals of the project were to develop a WSN for widespread use in historic structures that would make it possible to monitor the response and to provide a convenient method of condition assessment. To ensure a thorough investigation, three field studies were conducted: Frankford Church, St. Paul Lutheran and the Johanniskirche. In the Frankford Church, the wireless sensor network was tested for its ability to measure tilt in the walls of a historic wood-framed structure during rehabilitation to level the foundations. St. Paul Lutheran investigated the WSNs application for a historic masonry structure with timber-framed roof to detect tilt in the walls during foundation underpinning and floor slab replacement. At the Johanniskirche, data from an existing WSN was used to create a moisture migration risk assessment tool for near real-time structural health monitoring.

The wireless sensor network was developed and configured for remote access capabilities. It was then applied at both the Frankford Church and St. Paul Lutheran before the start of construction and remained on the structures until the foundation work was completed. The results indicate the motes have low sensitivity, but they were able to detect long-term trends in the tilt of the walls. Therefore, this approach is feasible to monitor tilt in the walls of historic structures under rehabilitation.

At the Johanniskirche, the results show that it is realistic to monitor climate conditions of historic structures under rehabilitation. Implementation of this risk assessment tool will help predict condensation events and prevent future damage to historic structures and the moisture migration protocol developed at the Johanniskirche provides a good basis for further investigation.

In the future, this technology should be used in conjunction with structural analysis software to determine acceptable tilt thresholds for the historic fabric of any structure on which the WSN is implemented. To be most helpful to structural engineers and preservationists alike, this information should then be formatted for use in real-time analysis so that the historic structure's supervisor will be alerted if the tilt exceeds the allowable levels. It is also recommended that motes with higher sensitivity be used to measure tilt in future endeavors. As previously noted, the development of energy saving algorithms to decrease energy consumption and efficient energy harvesting methods based on solar, vibration or thermal energy could greatly improve the WSN's performance.

As previously mentioned, field studies addressing climate conditions which implement the suggested corrective actions will serve to further optimize the criteria and validate conclusions. It is recommended that future installations to include output plots with indicators for appropriate condensation risk minimization actions (i.e., red, yellow and green lights that correspond to necessary actions). The incorporation of short term weather forecasts to predict future risk conditions could also be a valuable asset.

REFERENCES

Analog Devices. (2000). “Low-Cost ±2g Dual-Axis Accelerometer with Duty Cycle Output.” <http://www.analog.com> (October 10, 2008).

Bastianini, F., Sarvestani, S. S., Nanni, A., Plessi, V., and Galati, N. (2007). “An Autonomous Networked Wireless Device for Structural Health Monitoring.” *Proceedings of the 3rd International Conference on Structural Health Monitoring of Intelligent Infrastructure*, Vancouver, British Columbia, Canada.

Bischoff, R., Feltrin, G., Meyer, J., and Matavalli, M. (2007). “Data Processing and Management Aspects of Wireless Sensor Networks for Structural Health Monitoring.” *Proceedings of the 3rd International Conference on Structural Health Monitoring of Intelligent Infrastructure*, Vancouver, British Columbia, Canada.

Blaise, J.-Y., De Luca, L., and Dudek, I. (2008). "Can Architectural Shapes Help Deciphering Data and Structuring Information? An Attempt through Case Studies." *Proceedings of CHRESP: 8th EC Conference on Sustaining Europe’s Cultural Heritage*, Ljubljana, Slovenia.

Bryson, L. S., Barnes, A. and Lutz, T. (2009). "Deformation Obtained from Acceleration Data Using Wireless Sensor Motes.” *Proceedings of the 4th International Conference on Structural Health Monitoring of Intelligent Infrastructure* (SHMII-4), Zurich, Switzerland.

Chen, Y.-M., and Lin, C.-Y. (2007). "Dynamic Simulation of Wireless Structural Monitoring System Using Petri Nets." *Proceedings of the 3rd International Conference on Structural Health Monitoring of Intelligent Infrastructure*, Vancouver, British Columbia, Canada.

Cinque, M., Cotroneo, D., DeCaro, G. and Pelella, M. (2006). "Reliability Requirements of Wireless Sensor Networks for Dynamic Structural Monitoring." *Supplemental Volume of the International Conference on Dependable Systems and Networks* (DSN), Philadelphia, PA.

Fisher, C. (2005). "The Virginia Capitol's Extreme Renovation." *Construction*, 72(22), 6.

Gao, Y., and Spencer, B.F. (2008). "Structural Health Monitoring Strategies for Smart Sensor Networks." *Newmark Structural Laboratory Report Series* (NSEL Report Series ISSN 1940-9826) Newmark Structural Engineering Laboratory, University of Illinois at Urbana-Champaign, Champaign, IL.

Geva, A. (2009). "The Utility of Computerized Energy Simulations in the Study of Religious Identity." *Proceedings of the 3rd International Congress on Construction History*. Cottbus, Germany.

Glaser, S. D., Shoureshi, R. A., and Pescovitz, D. (2005). "Frontiers in Sensors and Sensing Systems." *Smart Structures & Systems*, 1, 103-120.

Gurlitt, C. (1910). *Beschreibende Darstellung der älteren Bau- und Kunstdenkmäler des Königreichs Sachsen*, Dresden: C. C. Meinhold und Söhne.

Hocker, E. (2010). "Maintaining a Stable Environment: Vasa's New Climate-Control System." *APT Bulletin*, 41(2-3), 3-9.

Hollar, S. (2000). "COTS Dust." M.S. thesis, University of California at Berkeley, Berkeley, CA.

Hurlebaus, S. and Gaul, L. (2006). "Smart Structure Dynamics." *Mechanical Systems and Signal Processing*, (Review paper), 20(2), 255-281.

Kijewski-Correa, T., Haenggi, M., and Antsaklis, P. (2006). "Multi-scale Wireless Sensor Networks for Structural Health Monitoring." *Proceedings of the 17th Analysis and Computation Specialty Conference*, University of Notre Dame, Notre Dame, IN.

Krüger, M. (2010). Personal Communication. University of Stuttgart, Stuttgart, Germany.

Krüger, M., Grosse, C.U., Bachmaier, S.A., and Willeke, J. (2010). "Wireless Monitoring of the Johanniskirche in Schwäbisch Gmünd." *Proceedings of the International Workshop on Preservation of Heritage Structures Using ACM and SHM* (CSHM-3), Ottawa-Gatineau, Canada.

Lammert, R. (2010). "Brief History." *Texas Wendish Heritage Society.* <http://texaswendish.org/BriefHistory.aspx> (March 5, 2010).

Lynch, J.P. and Loh, K.J. (2006). "A Summary Review of Wireless Sensors and Sensor Networks for Structural Health Monitoring." *The Shock and Vibration Digest*, 38(2), 91-128.

Nielsen, G.R. (1989). *In Search of a Home: 19th Century Wendish Immigration*. College Station, TX: Texas A&M University Press.

Reinisch, C., Kastner, W., Neugschwandtner, G. and Granzer, W. (2007). "Wireless Technologies in Home and Building Automation." *Proceedings of the IEEE International Conference on Industrial Informatics*, Vienna, Austria.

Reyer, M. (2007). "Design of a Wireless Sensor Network for Structural Health Monitoring of Bridges." M.S. thesis, Texas A&M University, College Station, TX.

Reyer, M., Mander, J.B. and Hurlebaus, S. (2009). "Design of a Wireless Sensor Network for Structural Health Monitoring of Bridges." *Mechanical Systems and Signal Processing*, (Under review).

Sensirion. (2009). "Introduction to Humidity: Basic Principles on Physics of Water Vapor." <http://www.sensirion.com> (June 11, 2010).

SmartMote. (2010). "Johanniskirche." <http://www.smartmote.de/Johanniskirche/Johanniskirche.html> (July 30, 2010).

SMooHS: Smart Monitoring of Historic Structures. (2010). "Objectives." <http://www.smoohs.eu> (July 5, 2010).

Sohn, H., Worden, K., and Farrar, C.R. (2002). "Statistical Damage Classification under Changing Environmental and Operational Conditions." *Journal of Intelligent Material Systems and Structures*, 13, 561-574.

St. Paul Lutheran. (1980). *St. Paul Lutheran, Serbin, Texas: A brief history.* [Pamphlet]. Serbin, TX.

St. Paul Lutheran. (2004). *St. Paul Lutheran, Serbin, Texas: A brief history.* [Pamphlet]. Serbin, TX.

St. Paul Lutheran (2010). *Serbin Church Restoration Project, Serbin, Texas.* <http://serbinchurchrestoration.blogspot.com> (April 30, 2010).

Staley, R. (2008). Personal Communication. Texas A&M University, College Station, TX.

Swartz, R.A., Jung, D., Lynch, J.P., Wang, Y., Shi, D. and Flynn, M.P. (2005). "Design of a Wireless Sensor for Scalable Distribution In-Network Computation in a Structural Health Monitoring System." *Proceedings of the 5th International Workshop on Structural Health Monitoring*, Stanford, CA.

Tanner, N.A., Farrar, C.R., and Sohn, H. (2002). "Structural Health Monitoring Using Wireless Sensing Systems with Embedded Processing." *Proceedings of SPIE – NDE and Health Monitoring of Aerospace Materials and Civil Infrastructure*, Newport Beach, CA.

Tanner, N.A., Wait, J.R., Farrar, C.R., and Sohn, H. (2003). "Structural Health Monitor Using Modular Wireless Sensors." *Journal of Intelligent Material Systems and Structures*, 14, 43-56.

Weather Underground. (2009). "Weather History." <http://www.wunderground.com/history> (December 30, 2009).

Weeks, K.D. and Grimmer, A.E. (1995). *Secretary of the Interior's Standards for the Treatment of Historic Properties with Guidelines for Preserving, Rehabilitating, Restoring, and Reconstructing Historic Buildings*, Washington DC: U.S.

Department of the Interior, National Park Service, Cultural Resource Stewardship and Partnerships, Heritage Preservation Services.

Xu, N., Rangwala, S., Chintalapudi, K.K., Ganesan, D., Broad, A., Govindan, R., and Estrin, D. (2004). "A Wireless Sensor Network for Structural Monitoring." *ACM Conference on Embedded Networked Sensor Systems. SenSys '04.* Baltimore, MD.

APPENDIX A

FRANKFORD CHURCH DATA

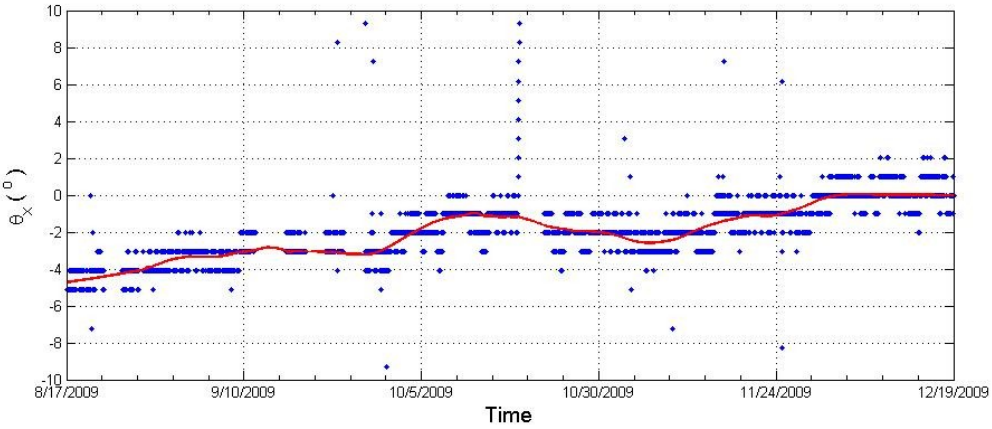

Figure A-1. Tilt of Mote 2 in $x-$direction

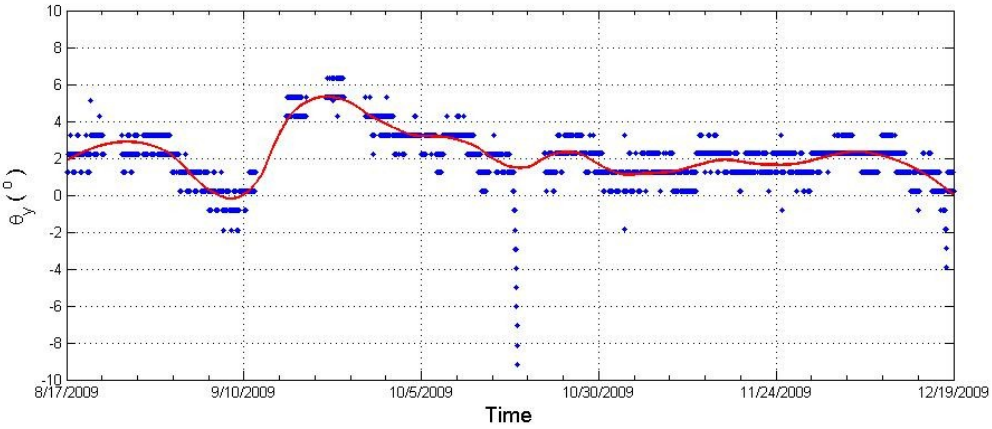

Figure A-2. Tilt of Mote 2 in $y-$direction

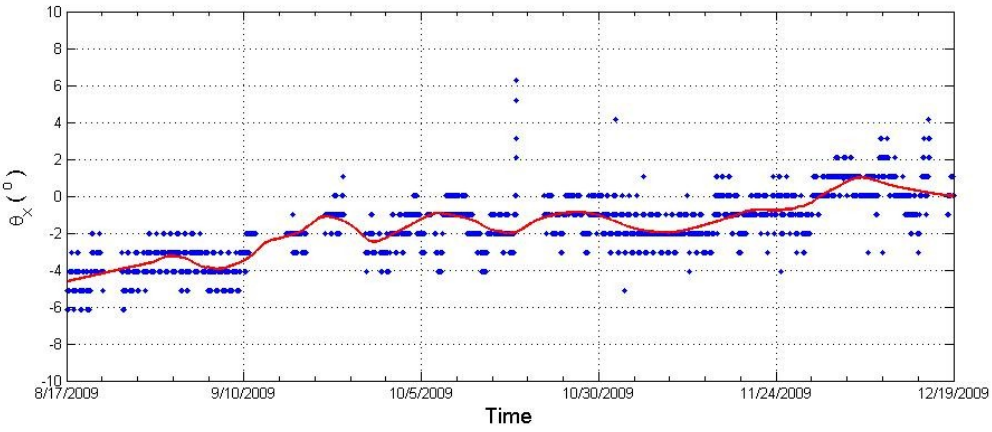

Figure A-3. Tilt of Mote 3 in $x-$direction

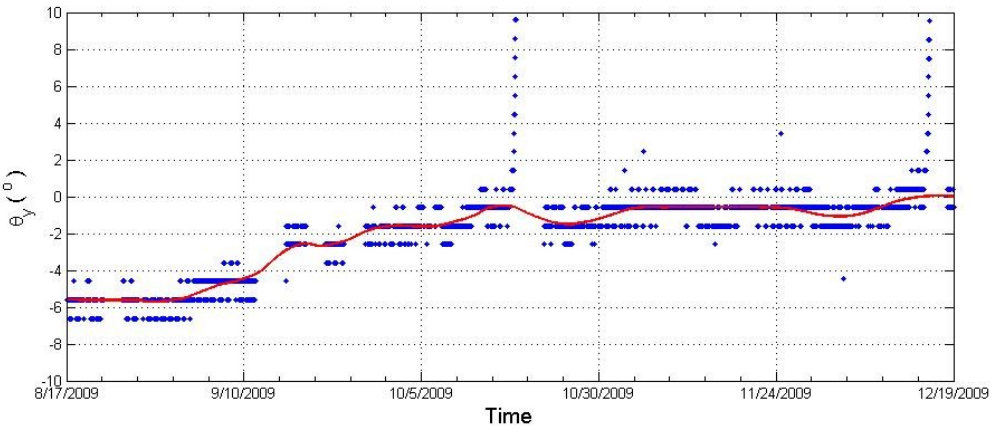

Figure A-4. Tilt of Mote 3 in $y-$direction

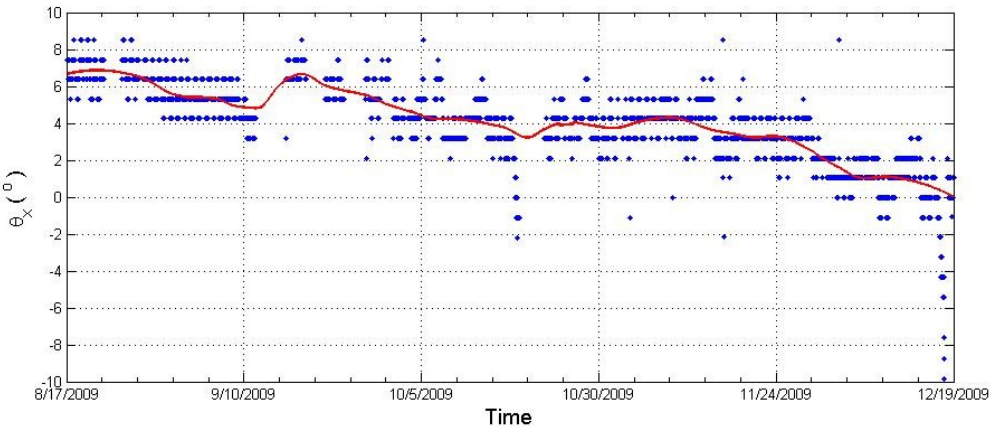

Figure A-5. Tilt of Mote 4 in $x-$direction

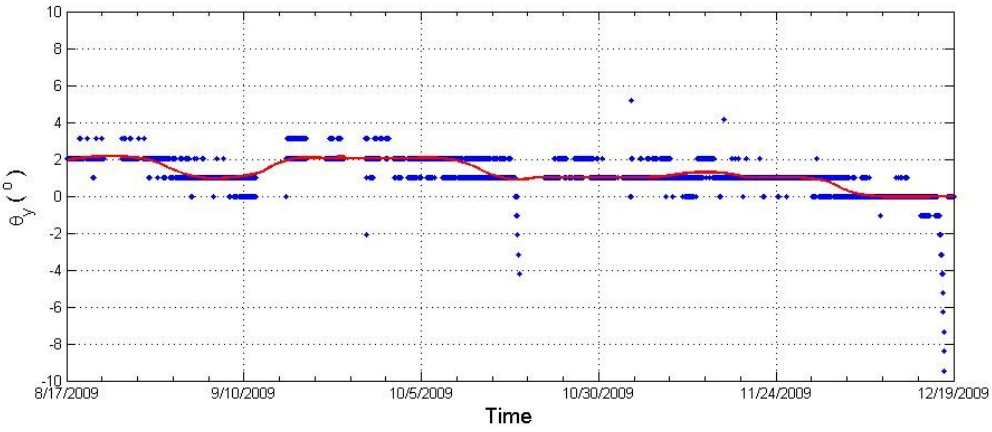

Figure A-6. Tilt of Mote 4 in $y-$direction

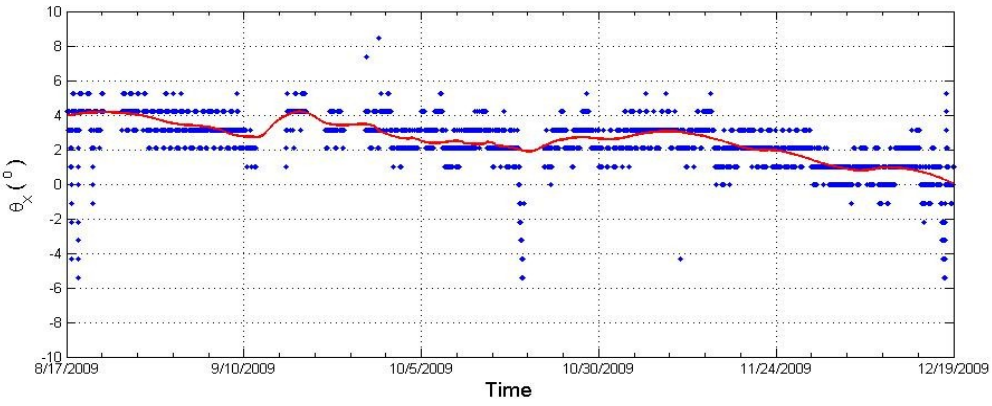

Figure A-7. Tilt of Mote 5 in $x-$direction

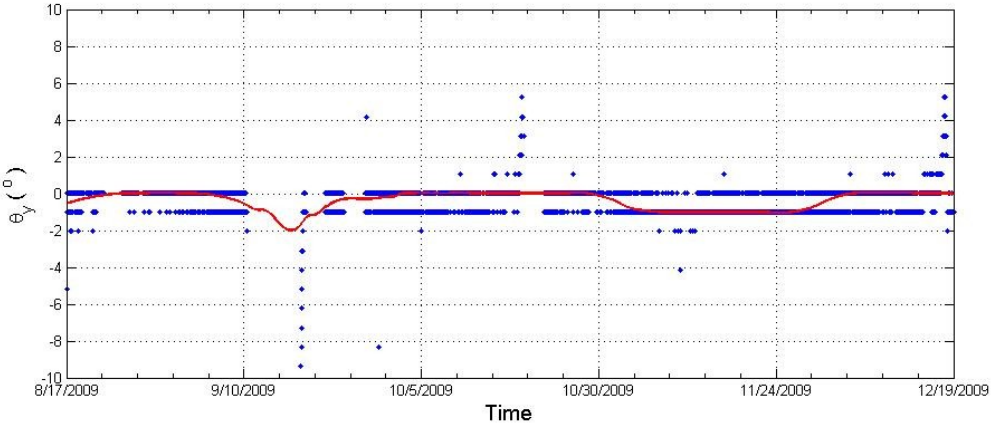

Figure A-8. Tilt of Mote 5 in $y-$direction

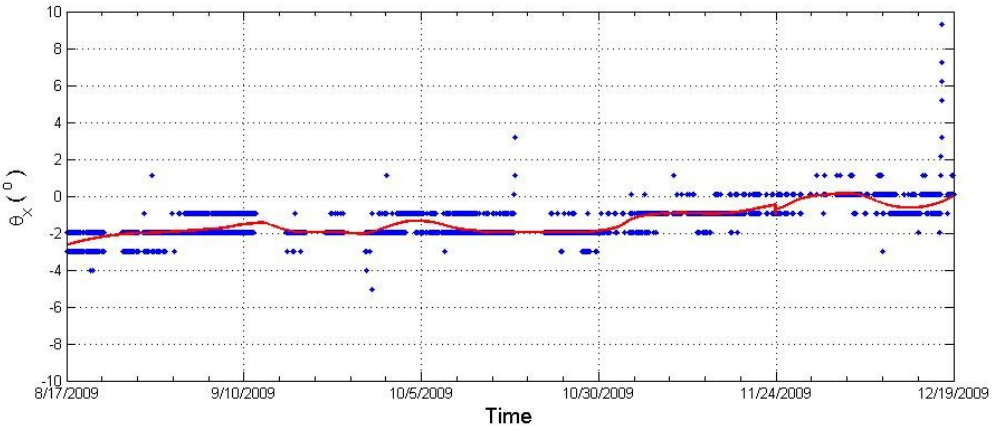

Figure A-9. Tilt of Mote 6 in $x-$direction

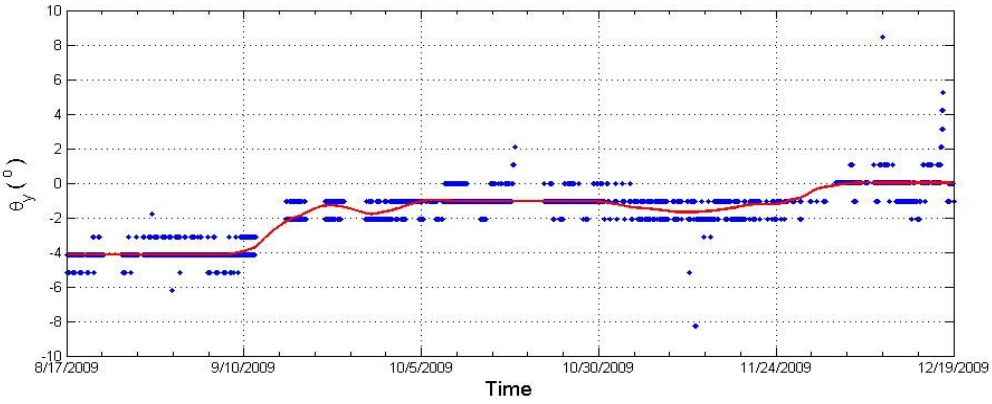

Figure A-10. Tilt of Mote 6 in $y-$direction

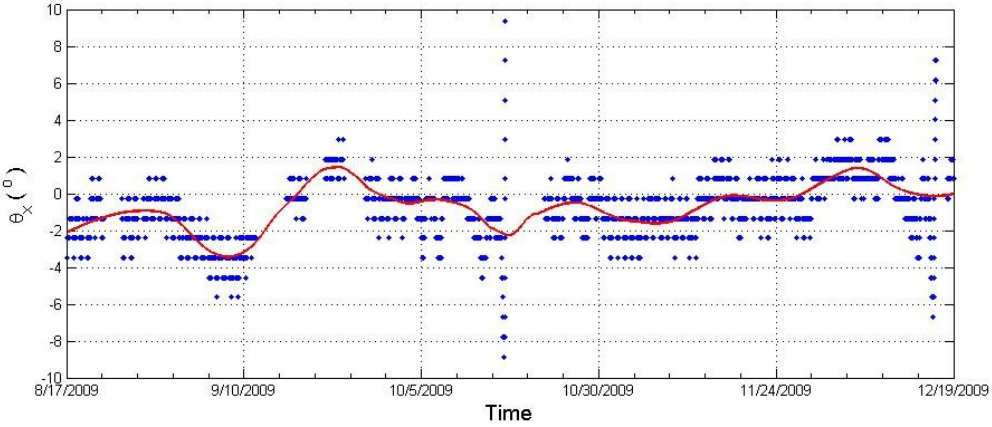

Figure A-11. Tilt of Mote 7 in $x-$direction

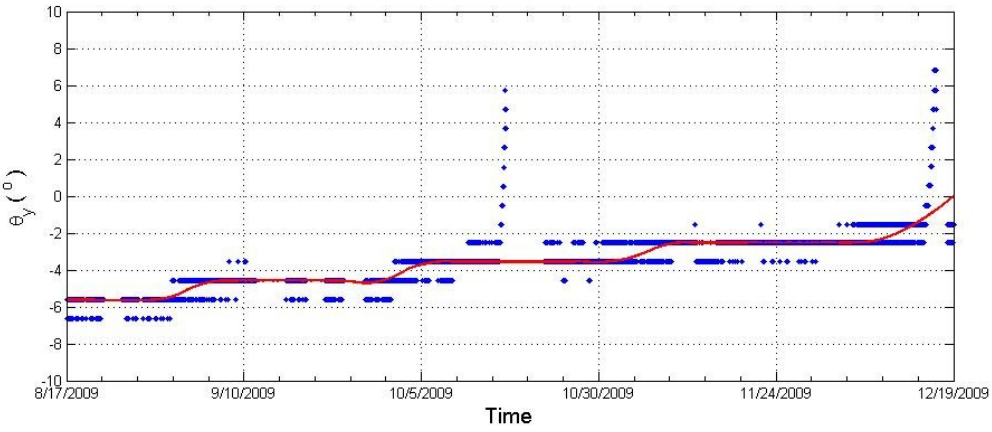

Figure A-12. Tilt of Mote 7 in $y-$direction

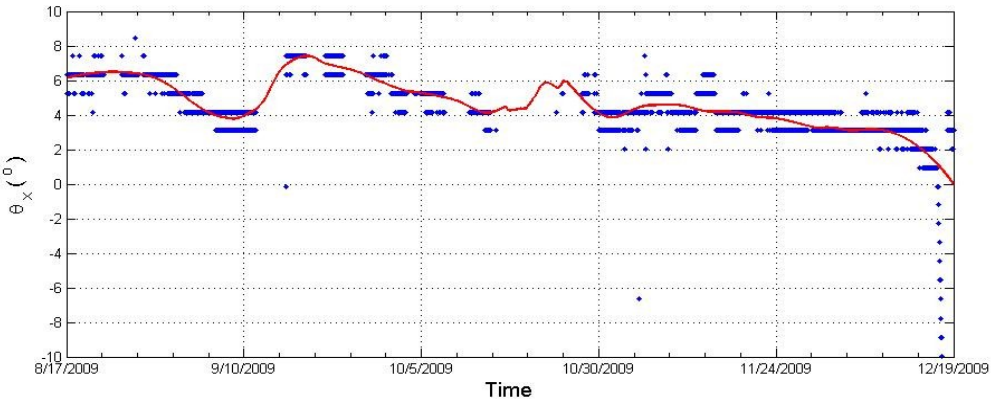

Figure A-13. Tilt of Mote 8 in $x-$direction

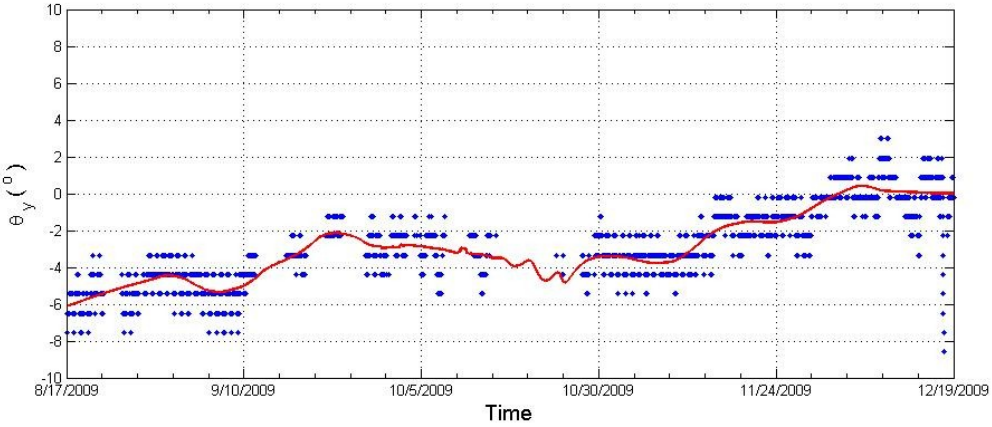

Figure A-14. Tilt of Mote 8 in $y-$direction

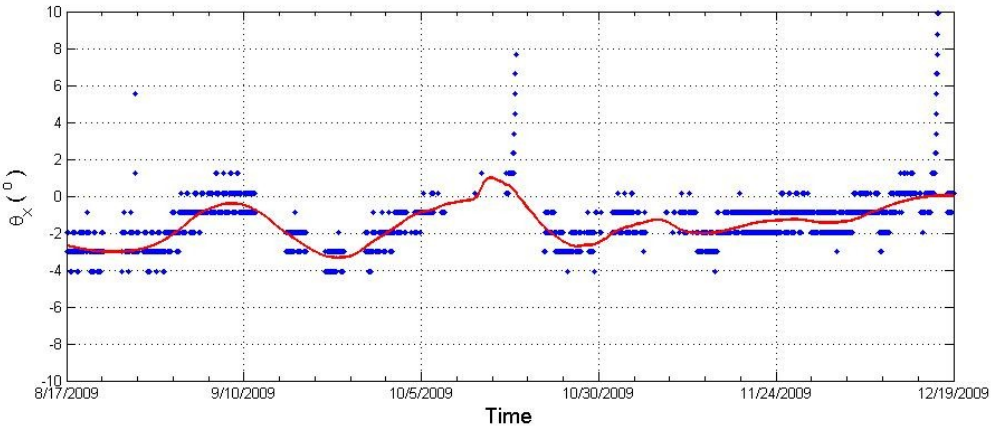

Figure A-15. Tilt of Mote 9 in $x-$direction

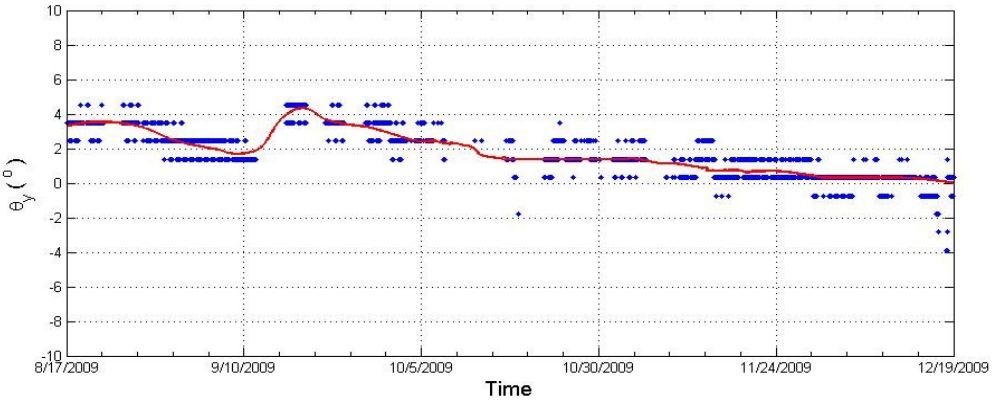

Figure A-16. Tilt of Mote 9 in $y-$direction

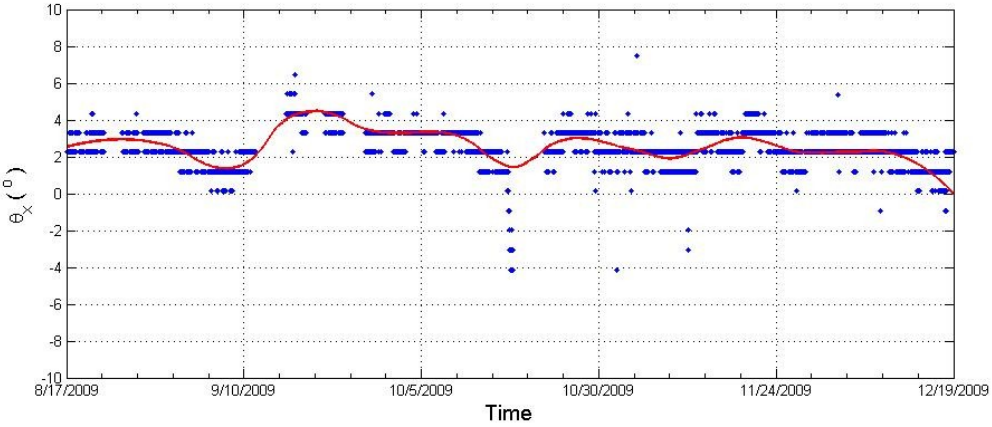

Figure A-17. Tilt of Mote 11 in $x-$direction

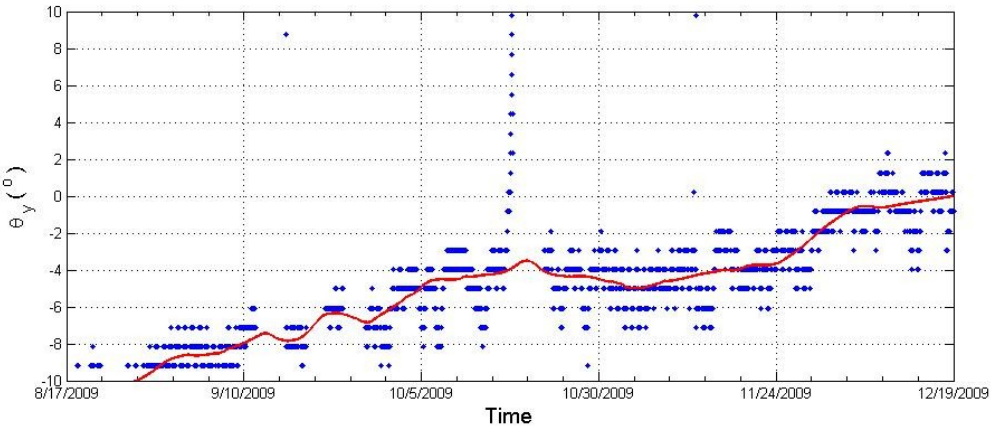

Figure A-18. Tilt of Mote 11 in $y-$direction

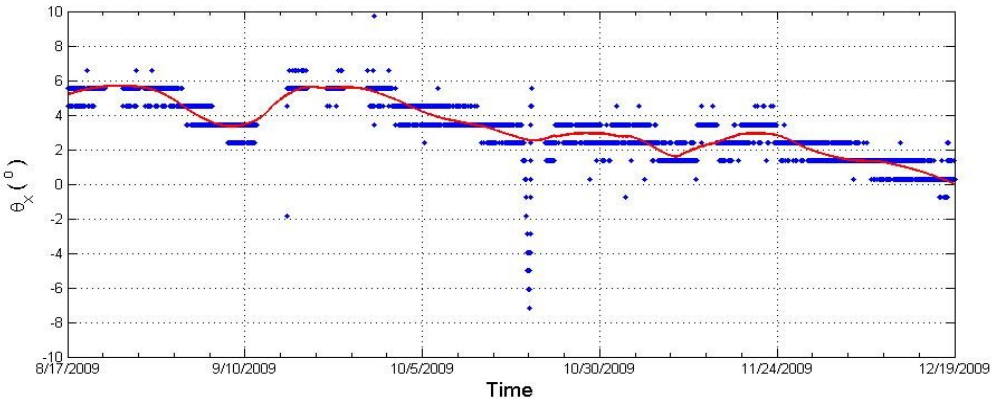

Figure A-19. Tilt of Mote 12 in $x-$direction

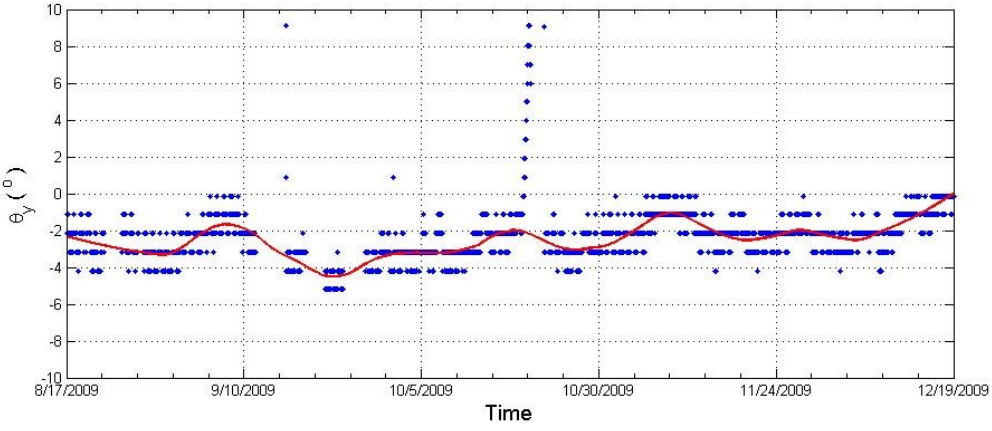

Figure A-20. Tilt of Mote 12 in $y-$direction

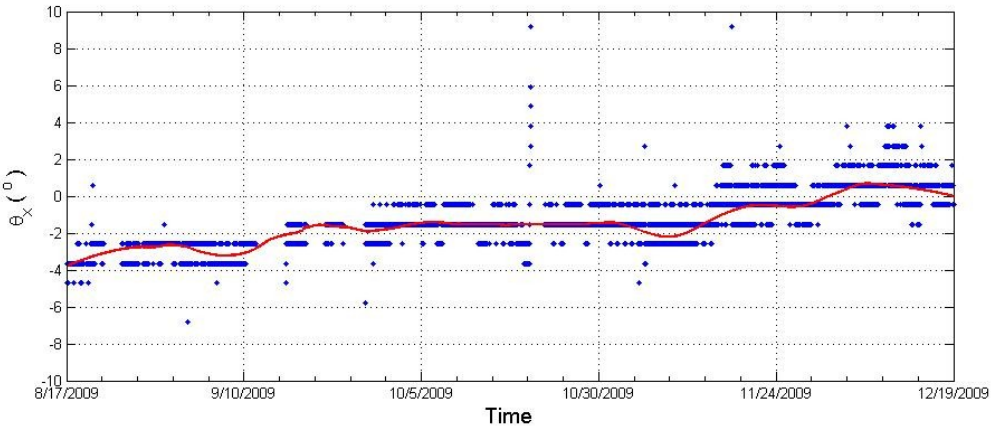

Figure A-21. Tilt of Mote 13 in $x-$direction

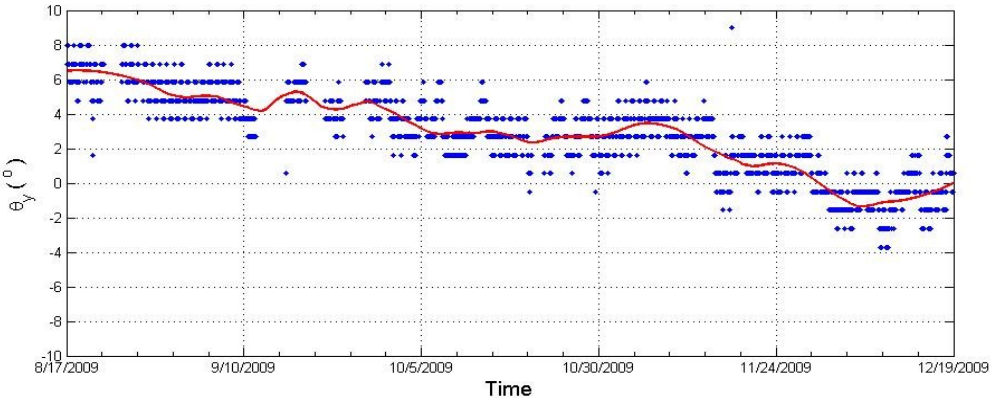

Figure A-22. Tilt of Mote 13 in $y-$direction

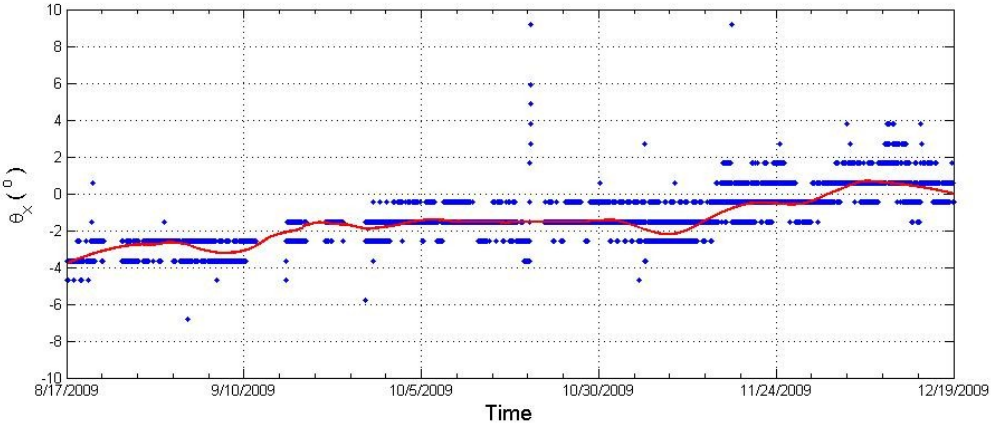

Figure A-23. Tilt of Mote 14 in $x-$direction

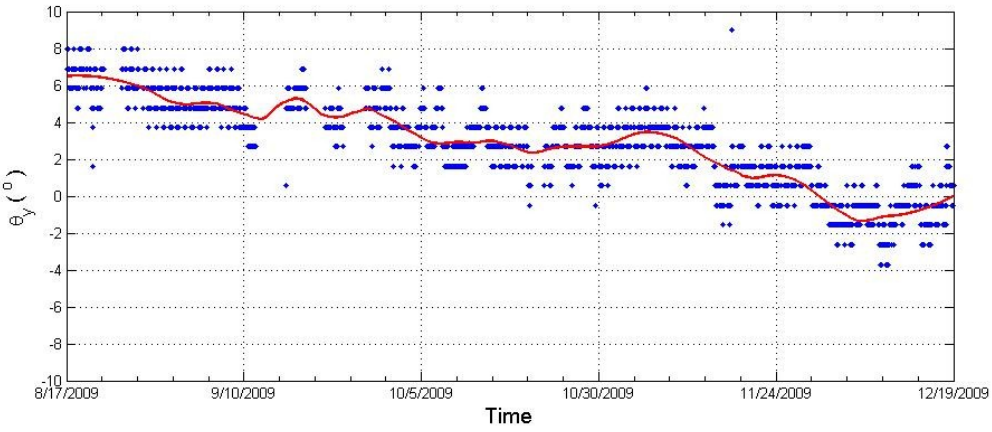

Figure A-24. Tilt of Mote 14 in $y-$direction

APPENDIX B

ST. PAUL LUTHERAN DATA

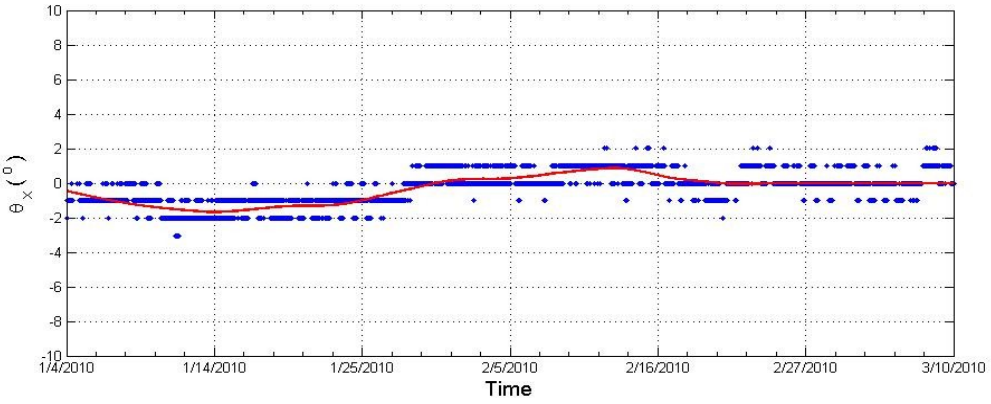

Figure B-1. Tilt of Mote 2 in $x-$direction

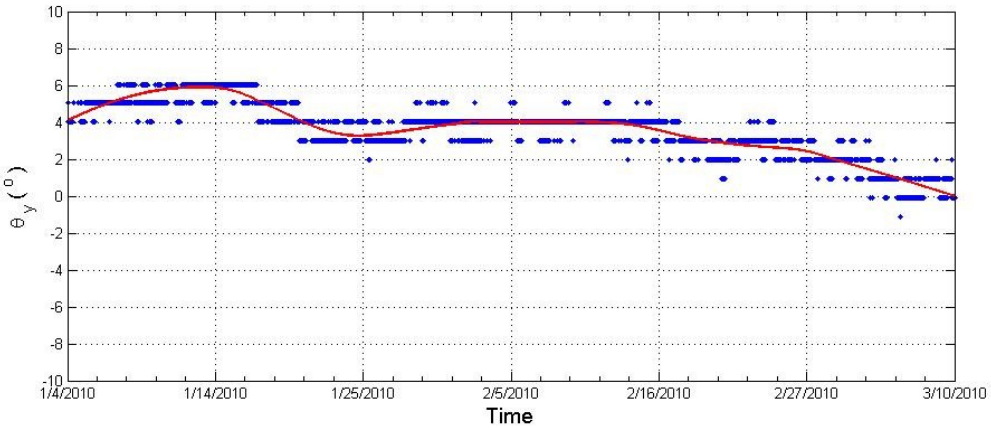

Figure B-2. Tilt of Mote 2 in $y-$direction

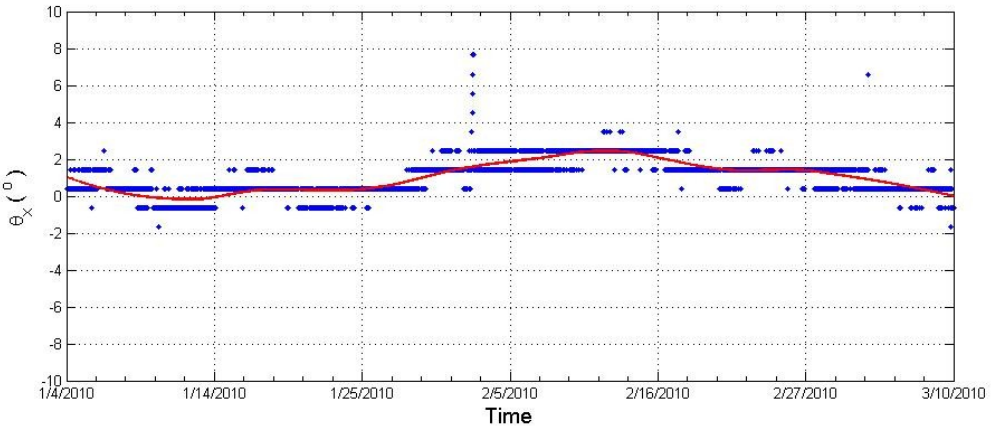

Figure B-3. Tilt of Mote 3 in $x-$direction

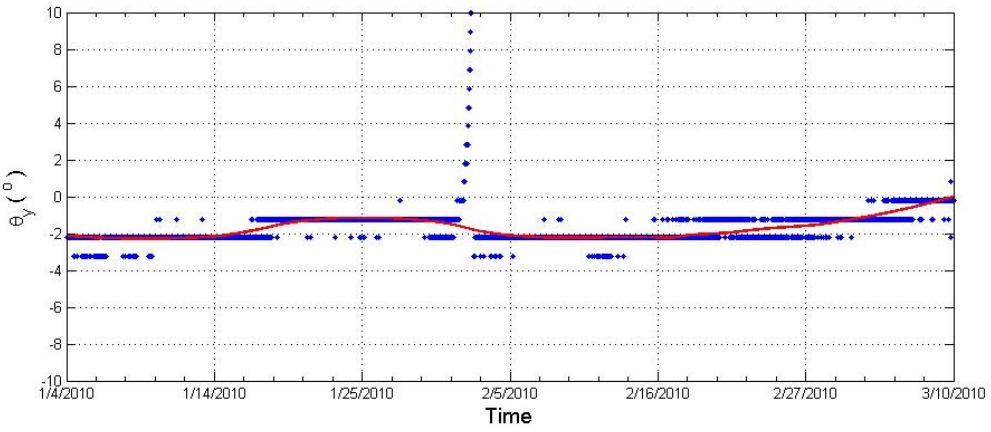

Figure B-4. Tilt of Mote 3 in $y-$direction

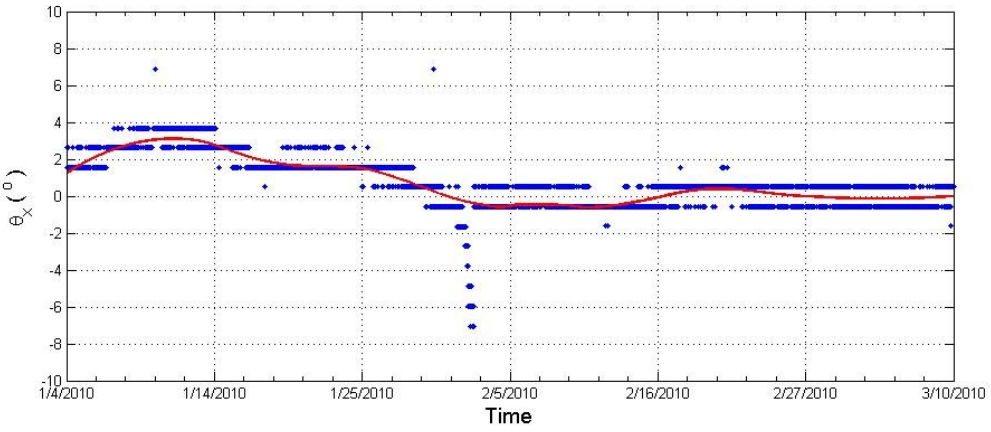

Figure B-5. Tilt of Mote 4 in $x-$direction

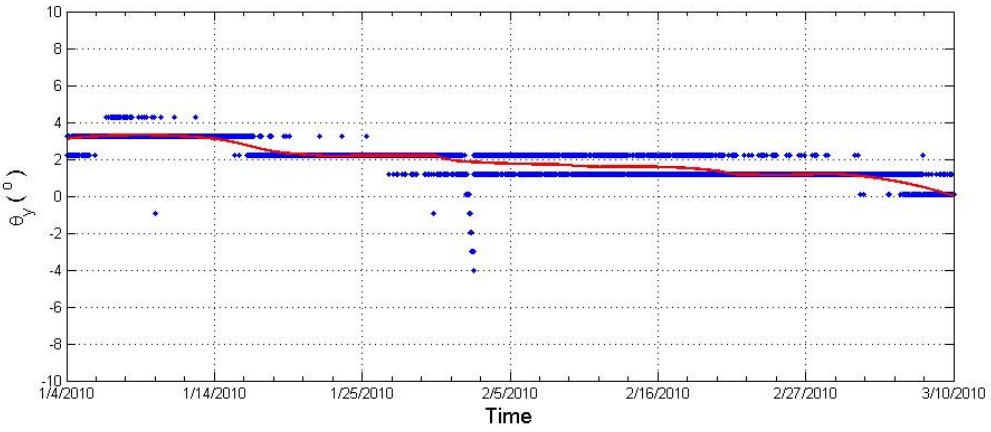

Figure B-6. Tilt of Mote 4 in $y-$direction

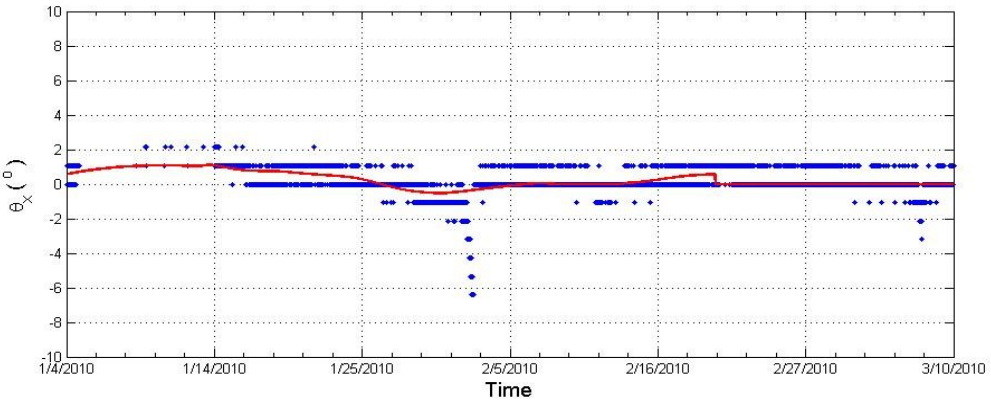

Figure B-7. Tilt of Mote 5 in $x-$direction

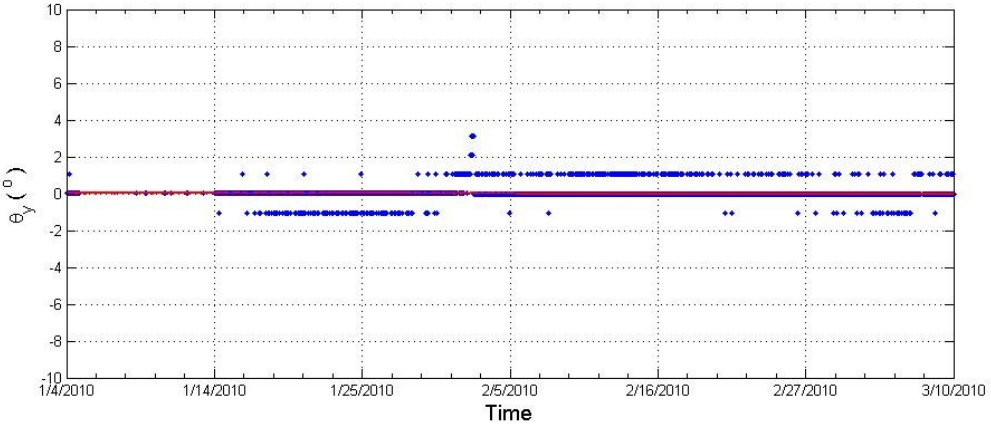

Figure B-8. Tilt of Mote 5 in $y-$direction

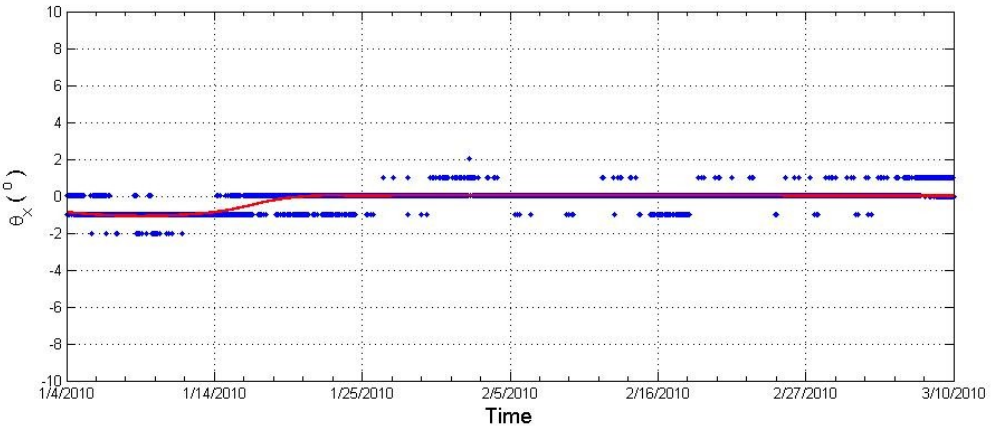

Figure B-9. Tilt of Mote 6 in $x-$direction

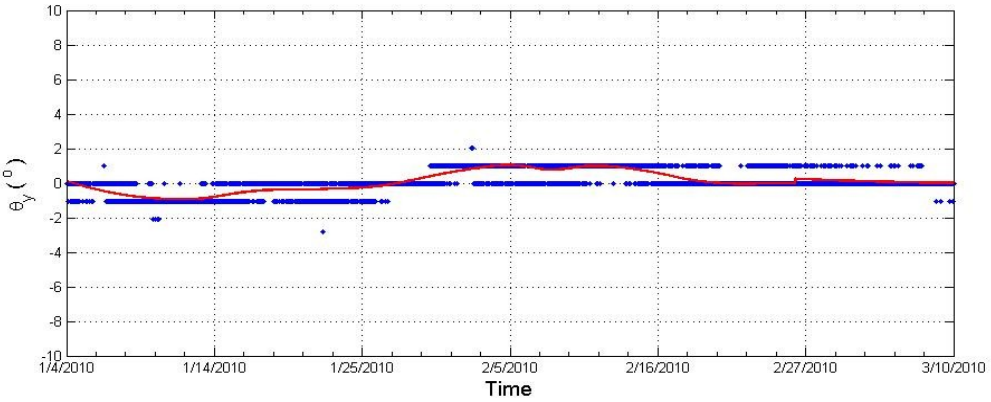

Figure B-10. Tilt of Mote 6 in $y-$direction

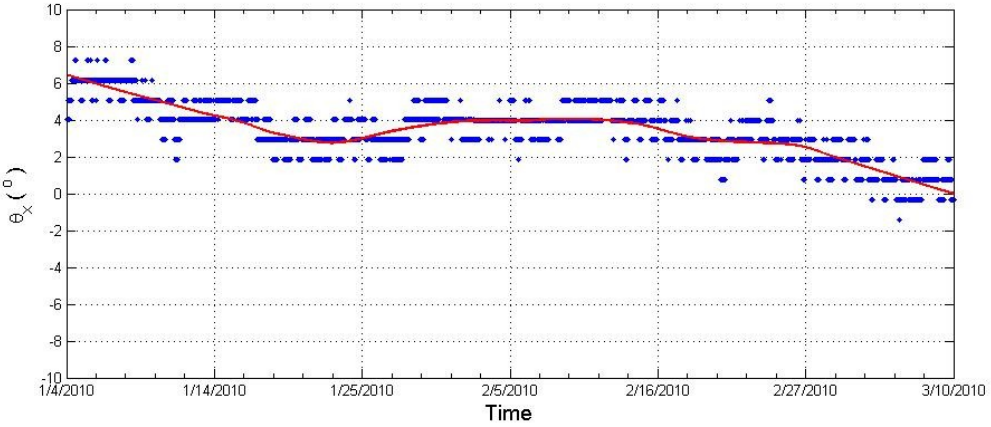

Figure B-11. Tilt of Mote 7 in $x-$direction

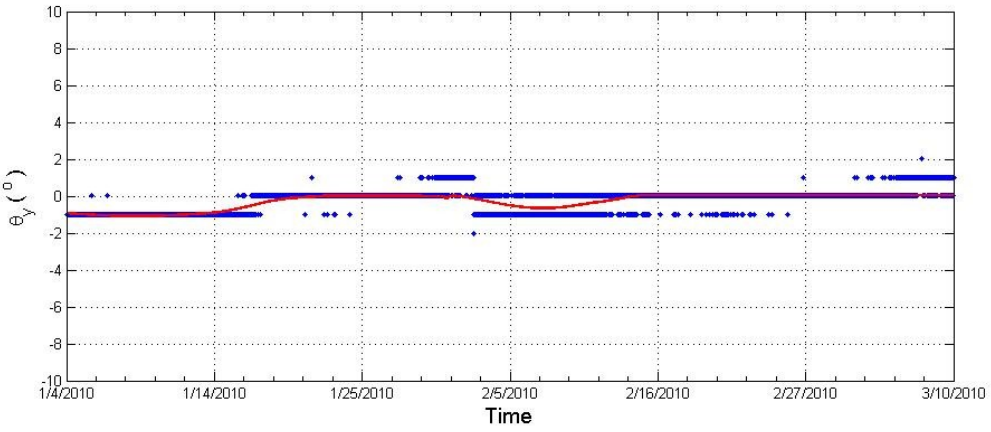

Figure B-12. Tilt of Mote 7 in $y-$direction

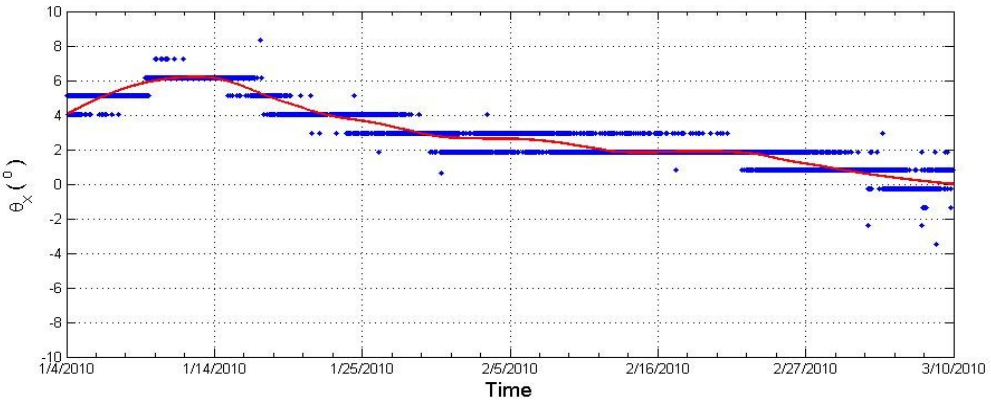

Figure B-13. Tilt of Mote 8 in $x-$direction

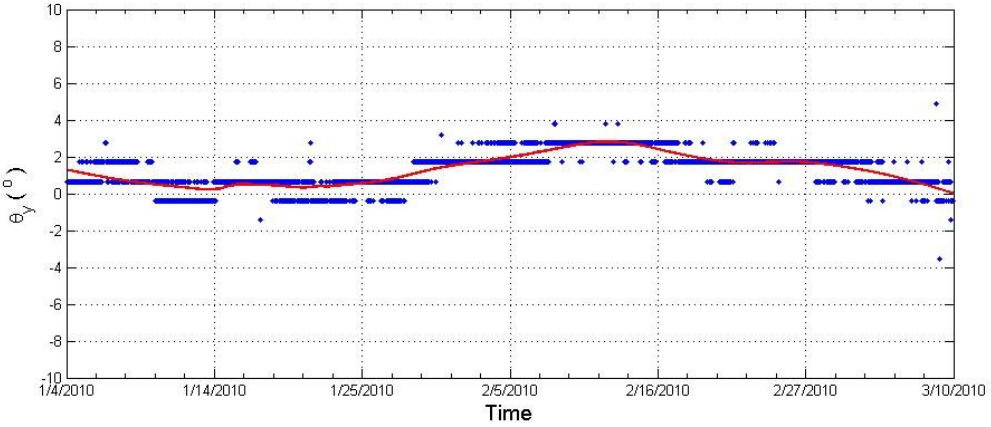

Figure B-14. Tilt of Mote 8 in $y-$direction

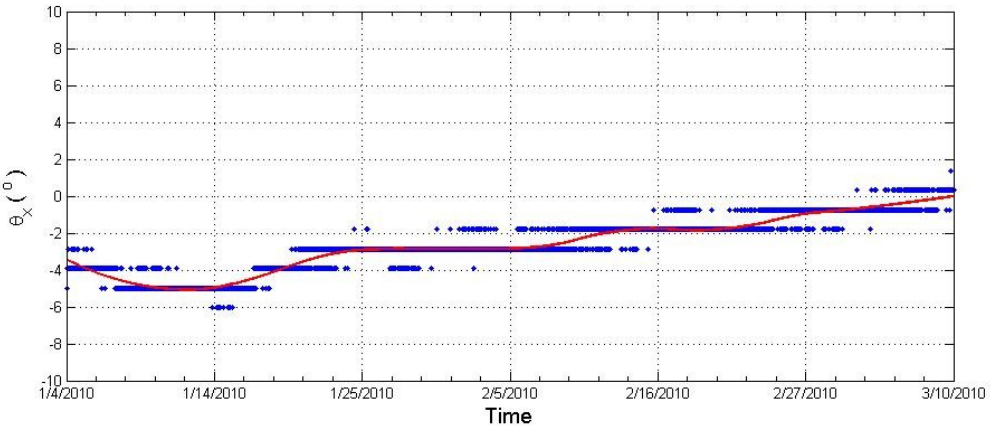

Figure B-15. Tilt of Mote 9 in $x-$direction

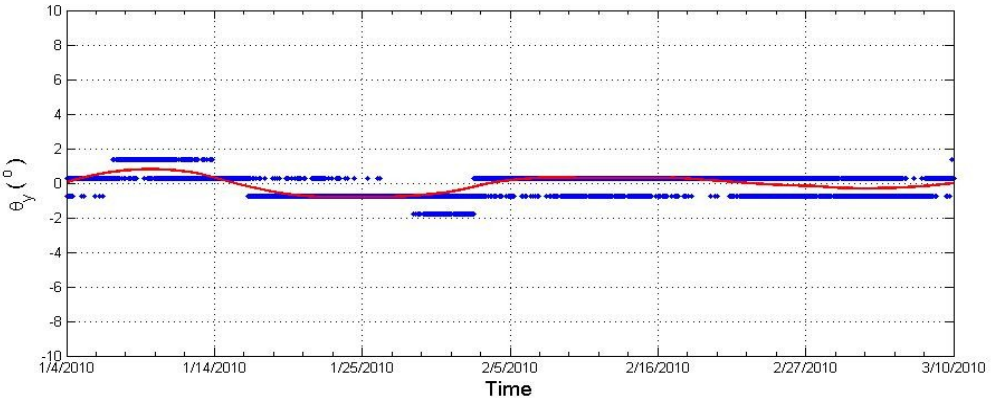

Figure B-16. Tilt of Mote 9 in $y-$direction

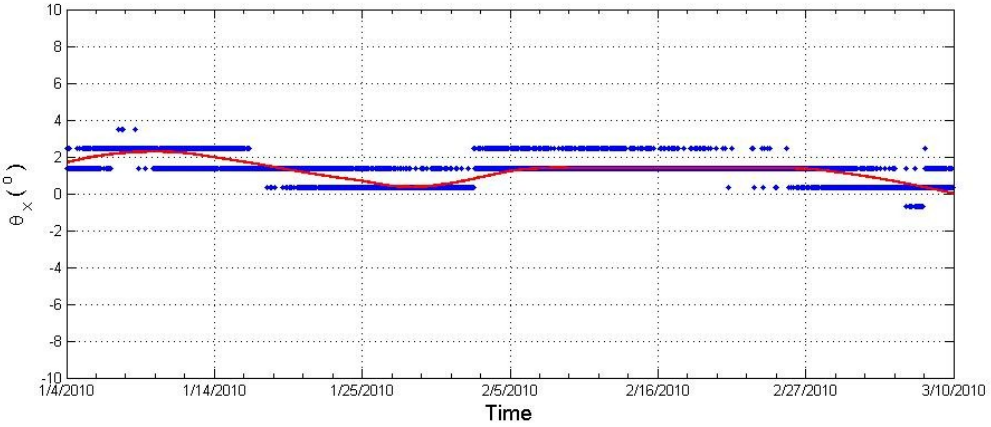

Figure B-17. Tilt of Mote 11 in $x-$direction

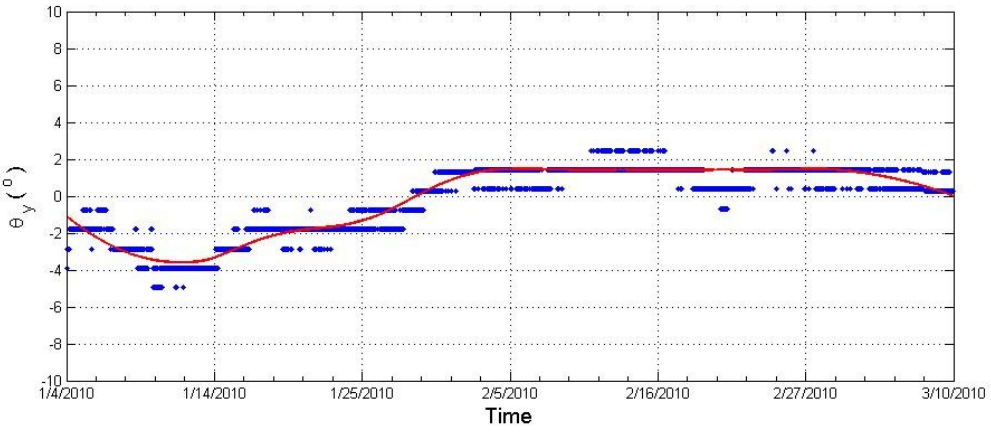

Figure B-18. Tilt of Mote 11 in $y-$direction

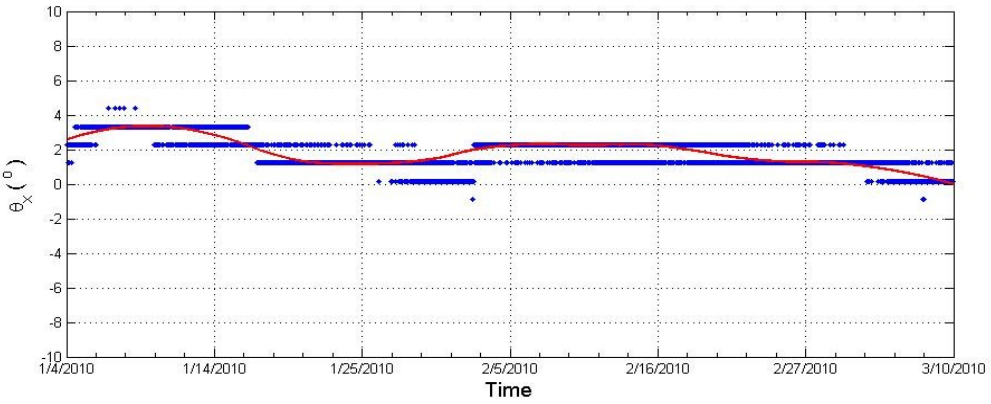

Figure B-19. Tilt of Mote 12 in $x-$direction

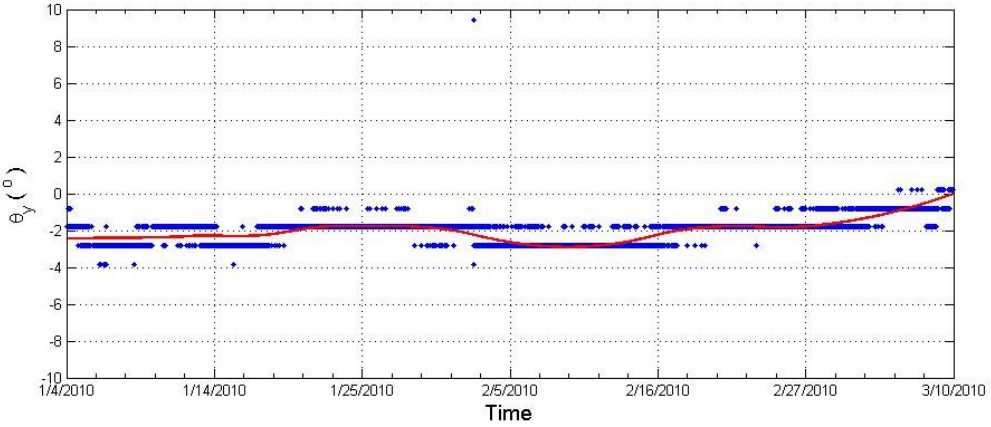

Figure B-20. Tilt of Mote 12 in $y-$direction

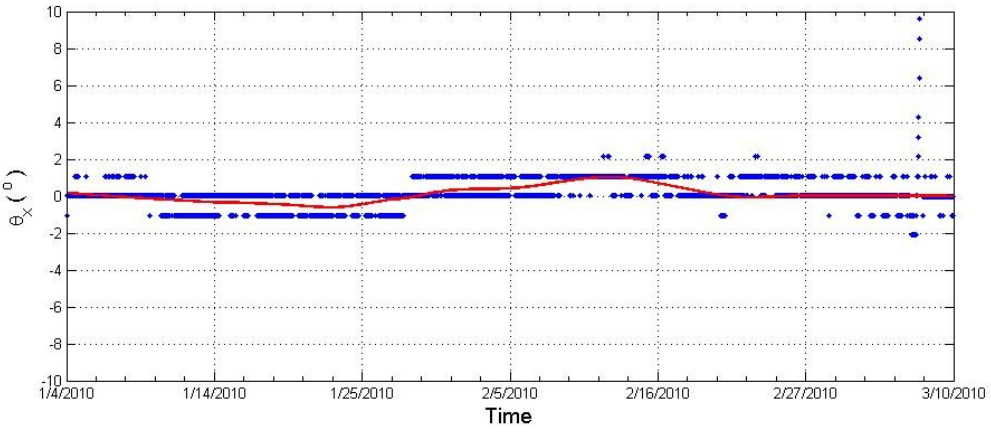

Figure B-21. Tilt of Mote 13 in $x-$direction

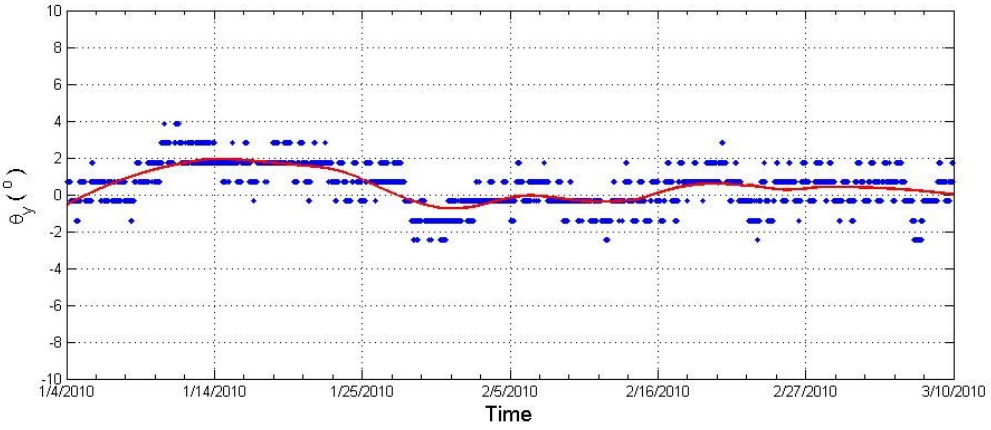

Figure B-22. Tilt of Mote 13 in $y-$direction

VITA

Name: Julie Marie Samuels

Address: Department of Civil Engineering
Texas A&M University
3136 TAMU
College Station, Texas 77843

Email Address: juliemsamuels@gmail.com

Education: B.S., Civil Engineering, Texas A&M University, 2008